Arteriosclerosis, Thrombosis, and Vascular Biology

BASIC SCIENCES

Cytokine-Mediated Degradation of the Transcription Factor ERG Impacts the Pulmonary Vascular Response to Systemic Inflammatory Challenge

Christopher M. Schafer, Silvia Martin-Almedina, Katarzyna Kurylowicz, Neil Dufton, Lourdes Osuna-Almagro, Meng-Ling Wu, Charmain F. Johnson, Aarti V. Shah, Dorian O. Haskard, Andrianna Buxton, Erika Willis, Kate Wheeler, Sean Turner, Magdalena Chlebicz, Rizaldy P. Scott, Susan Kovats, Audrey Cleuren, Graeme M. Birdsey, Anna M. Randi, Courtney T. Griffin

BACKGROUND: During infectious diseases, proinflammatory cytokines transiently destabilize interactions between adjacent vascular endothelial cells (ECs) to facilitate the passage of immune molecules and cells into tissues. However, in the lung, the resulting vascular hyperpermeability can lead to organ dysfunction. Previous work identified the transcription factor ERG (erythroblast transformation-specific–related gene) as a master regulator of endothelial homeostasis. Here we investigate whether the sensitivity of pulmonary blood vessels to cytokine-induced destabilization is due to organotypic mechanisms affecting the ability of endothelial ERG to protect lung ECs from inflammatory injury.

METHODS: Cytokine-dependent ubiquitination and proteasomal degradation of ERG were analyzed in cultured HUVECs (human umbilical vein ECs). Systemic administration of TNFα (tumor necrosis factor alpha) or the bacterial cell wall component lipopolysaccharide was used to cause a widespread inflammatory challenge in mice; ERG protein levels were assessed by immunoprecipitation, immunoblot, and immunofluorescence. Murine *Erg* deletion was genetically induced in ECs (*Erg*$^{fl/fl}$;*Cdh5[PAC]-Cre*^{ERT2}), and multiple organs were analyzed by histology, immunostaining, and electron microscopy.

RESULTS: In vitro, TNFα promoted the ubiquitination and degradation of ERG in HUVECs, which was blocked by the proteasomal inhibitor MG132. In vivo, systemic administration of TNFα or lipopolysaccharide resulted in a rapid and substantial degradation of ERG within lung ECs but not ECs of the retina, heart, liver, or kidney. Pulmonary ERG was also downregulated in a murine model of influenza infection. *Erg*$^{fl/fl}$;*Cdh5(PAC)-Cre*^{ERT2} mice spontaneously recapitulated aspects of inflammatory challenges, including lung-predominant vascular hyperpermeability, immune cell recruitment, and fibrosis. These phenotypes were associated with a lung-specific decrease in the expression of *Tek*—a gene target of ERG previously implicated in maintaining pulmonary vascular stability during inflammation.

CONCLUSIONS: Collectively, our data highlight a unique role for ERG in pulmonary vascular function. We propose that cytokine-induced ERG degradation and subsequent transcriptional changes in lung ECs play critical roles in the destabilization of pulmonary blood vessels during infectious diseases.

GRAPHIC ABSTRACT: A graphic abstract is available for this article.

Key Words: capillary permeability ■ endothelial cells ■ inflammation ■ lung ■ proteolysis ■ transcription factors

Correspondence to: Courtney T. Griffin, Oklahoma Medical Research Foundation, Oklahoma City, OK 73104, Email courtney-griffin@omrf.org; or Anna M. Randi, Imperial College London, London, United Kingdom, Email a.randi@imperial.ac.uk

Supplemental Material is available at https://www.ahajournals.org/doi/suppl/10.1161/ATVBAHA.123.318926.
For Sources of Funding and Disclosures, see page 1426.

Arterioscler Thromb Vasc Biol is available at www.ahajournals.org/journal/atvb

Nonstandard Abbreviations and Acronyms

ARDS	acute respiratory distress syndrome
CD31	cluster of differentiation 31
EC	endothelial cell
ERG	erythroblast transformation-specific–related gene
HA	hemagglutinin
HUVEC	human umbilical vein endothelial cell
IL	interleukin
LPS	lipopolysaccharide
MPO	myeloperoxidase
qPCR	real-time quantitative reverse transcription PCR
RNAPol2	RNA polymerase II
TNFα	tumor necrosis factor alpha

Highlights

- The endothelial transcription factor ERG (erythroblast transformation-specific–related gene) is rapidly downregulated predominantly in mouse lungs after systemic inflammatory challenge.
- TNFα (tumor necrosis factor alpha) promotes ubiquitination and degradation of ERG.
- Mice with endothelial *Erg* deletion spontaneously develop lung-predominant vascular hyperpermeability, immune cell recruitment, and fibrosis.

Vascular endothelial cells (ECs) form a dynamic, semipermeable interface between blood and tissues. Therefore, ECs are among the first responders to systemic inflammatory challenges such as sepsis—a life-threatening condition in which bacterial infection of the blood triggers the release of abundant cytokines into the circulation.[1,2] In response to these stimuli, ECs adopt inflammatory phenotypes and participate in the initiation of local tissue responses.[3,4] By adjusting expression of cell surface proteins, activated ECs weaken their own intercellular junctions while also promoting interactions with circulating leukocytes.[5] Collectively, these alterations destabilize blood vessels, leading to vascular hyperpermeability that allows immune cell extravasation and the exchange of immune molecules between the blood and peripheral tissue. However, failure to resolve vascular inflammation in a timely manner results in excessive immune cell infiltration, pathological tissue edema, and ultimately organ dysfunction.[6]

For unclear reasons, blood vessels within the lung are particularly prone to pathological hyperpermeability in many inflammatory diseases.[7–10] During bacterial and viral infections, compromised vascular stability undermines pulmonary function by impairing efficient gas exchange between the dense capillary network and underlying airway epithelial cells.[6,11–13] This can result in acute respiratory distress syndrome (ARDS), which is associated with high mortality rates.[8,11] Since treatments that target the pathogenesis of ARDS are currently lacking, patients are typically put on ventilators to support their reduced respiratory capacity.[14] Mounting experimental evidence suggests that stabilization of microvascular ECs may be a useful approach to alleviate pulmonary dysfunction.[6,15–17] Yet, refinement of these therapeutic strategies requires a deeper understanding of mechanisms responsible for the lung's unique predisposition to vascular dysfunction under inflammatory challenges.

Here, we demonstrate how organotypic regulation of the endothelial erythroblast transformation-specific family transcription factor ERG (erythroblast transformation-specific–related gene) coordinates a vascular inflammatory response within the lung. ERG functions as a gatekeeper that suppresses vascular inflammation.[18–23] In turn, ERG is regulated by proinflammatory stimuli at the transcriptional and posttranslational levels. In addition, recent reports demonstrate the capacity for proteolytic ERG degradation in cultured ECs, although the in vivo contexts for such degradation are not fully understood.[24,25] In this study, we demonstrate ERG ubiquitination and proteasomal degradation in ECs following stimulation with the proinflammatory cytokine TNFα (tumor necrosis factor alpha) in vitro and in vivo. Unexpectedly, we found that cytokine-induced ERG degradation in vivo occurs preferentially in pulmonary ECs. Downregulation of ERG is similarly seen in the lungs of mice challenged with a bacterial wall component or with viral infection. Importantly, genetic deletion of *Erg* in ECs throughout the body results in more severe vascular hyperpermeability, immune cell recruitment, and fibrosis in the lung than in other organs, suggesting that cytokine-induced ERG degradation may account for the lung's unique susceptibility to inflammatory vascular dysfunction.

METHODS

The data that support the findings of this study are available from the corresponding authors upon reasonable request.

Mice

Mice used in this study include C57Bl/6J (No. 000664; The Jackson Laboratory), *Il1r1*^{flox} (No. 028398; The Jackson Laboratory),[26] *Tnfa*$^{-/-}$ (No. 003008; The Jackson Laboratory),[27] *Cdh5(PAC)-CreERT2* (gift of Ralf Adams, Max Planck Institute for Molecular Biomedicine; No. 13073; Taconic),[28] *VE-Cadherin-Cre* (No. 006137; The Jackson Laboratory),[29] and *Tie2-Cre* (No. 008863; The Jackson Laboratory).[30] EC-specific deletion of *Erg* was accomplished by crossing mice expressing *Cdh5(PAC)-CreERT2* with 2 independent *Erg*^{flox} mouse lines. For data presented in Figures 5 and 6, *Erg*^{flox} mice were a gift of Joshua Wythe (Baylor College of Medicine; No. 030988; The

Jackson Laboratory),[31] and gene deletion was accomplished by oral gavage of 100 µL of 20 mg/mL tamoxifen (No. T5648; Sigma) dissolved in peanut oil over 3 days. Mice were then returned to their cages for 3 to 4 weeks. For data presented in Figure 7, *Erg*^{flox} mice were generated in our laboratory and described in detail elsewhere[32]; deletion of *Erg* was induced in adult mice, between 6 and 8 weeks, by tamoxifen injection (5 injections of 0.5 mg daily). Genotyping for each allele was performed using the primers listed in Table S2. All mice were maintained on a C57Bl/6J background and were between 2 and 6 months of age when used for experiments. Genders of mice used for each experiment are listed in Table S4. Mice were euthanized using isoflurane overdose (5%) followed by cardiac exsanguination and dissection. All studies using animals were performed in accordance with the NIH (National Institutes of Health) Guide for the Care and Use of Laboratory Animals and were approved by the Institutional Animal Care and Use Committees at the Oklahoma Medical Research Foundation or were conducted with ethical approval from Imperial College London under UK Home Office in compliance with the UK Animals (Scientific Procedures) Act of 1986.

Lipopolysaccharide, MG132, and Proinflammatory Cytokine Treatment of Mice

Lipopolysaccharide (LPS), proinflammatory cytokines, and MG132 were administered to mice via intraperitoneal (LPS and MG132) or intravenous (LPS, TNFα, IL [interleukin]-1α, IL-1β, and IL-18) injection. Intraperitoneal LPS injection was performed using a 1- to 2-mg/mL stock solution of LPS (No. L3012; Sigma; resuspended in sterile 0.9% saline) that was administered to mice at a dosage of 4 or 10 mg/kg body weight (BW) for up to 72 hours. Pretreatment with MG132 was accomplished using a 20-mg/mL stock solution of MG132 (No. BML-PI102; Enzo Life Sciences; resuspended in DMSO [dimethyl sulfoxide]) that was diluted in 5% ethanol to a 0.5-mg/mL working stock, filter sterilized, and administered to mice at a dosage of 10 mg/kg BW for 3 hours before LPS administration. Intravenous injections of LPS, TNFα (No. 410-MT; R&D Systems), IL-1α (No. ab256050; Abcam), IL-1β (No. 401-ML; R&D Systems), or IL-18 (No. 9139-IL; R&D Systems) were performed via the retro-orbital sinus, as described previously.[33] Each compound was resuspended in sterile 0.9% saline from which 100 to 150 µL was injected into isoflurane-anesthetized mice at a final dosage of 1 mg/kg BW (LPS) or 50 µg/kg BW (TNFα, IL-1α, IL-1β, and IL-18). Mice were then returned to their cages for 3 hours before tissue collection.

Influenza Infection

Intratracheal influenza infection was performed on C57Bl/6J mice using a mouse-adapted A/Puerto Rico/8/1934 (PR8, H1N1) virus as described previously.[34] Mice were anesthetized by a single intraperitoneal injection of a ketamine (60 mg/kg BW)/xylazine (4.5 mg/kg BW) solution and then placed on an inclined surface to enable intratracheal administration of 30 µL of PBS containing either low (800 egg infective dose) or high (1050 egg infective dose) viral doses. Mice were then returned to their cages for 2 or 6 days, during which time they were monitored daily for signs of morbidity, such as weight loss.

Immunoblot

For immunoblot analysis of murine tissues, mice were perfused with 10 mL warm PBS using a Bio-Rad Econo Pump (at a flow rate of 1 mL/min) and a 23-g needle inserted into the left ventricle of the heart. Lung, heart, liver, kidney, and retina tissues were then collected, washed in PBS, and snap frozen in liquid N_2. Tissue samples were then lysed by sonication in RIPA (radio-immunoprecipitation assay) buffer (50 mM Tris-HCl [pH 7.4], 150 mM NaCl, 1% SDS, 1 mM EDTA, and 0.5% sodium deoxycholate) with 1 mM phenylmethylsulfonyl fluoride and protease inhibitor cocktail (No. P8340; Sigma) added just before use. Tissue lysates were centrifuged at 10 000*g* for 10 minutes at 4 °C to remove cell debris, and the protein concentrations of supernatants were determined using a BCA Protein Assay Kit (No. 23227; Thermo Scientific), following the manufacturer's instructions. Samples were then diluted to 5- to 10-mg/mL in PAGE running buffer (62.5 mM Tris-HCl [pH 6.8], 2% SDS, 10% glycerol, 5% β-mercaptoethanol, 0.002% bromophenol blue) and heated at 95 °C for 10 minutes. Protein samples (10–20 µg) were separated on 9% SDS-PAGE gels and then transferred to a PVDF (polyvinylidene fluoride) membrane that was blocked for 1 hour in 5% nonfat dry milk dissolved in TBST (tris-buffered saline with 0.1% Tween 20 detergent). Primary antibodies were diluted in 5% milk-TBST and incubated on membranes overnight at 4 °C with gentle agitation. Membranes were then washed 3× (15 minutes each) in TBST, and HRP (horseradish peroxidase)-conjugated secondary antibodies (diluted in 5% milk-TBST) were applied for 3 hours at 25 °C with gentle agitation. Secondary antibodies were detected using the ECL Western Blotting Detection Reagent (No. 95038-562; GE Healthcare). Immunoblot band densitometry and normalization to GAPDH expression was performed using the NIH ImageJ software.[35]

Tissue Section Imaging by Immunofluorescence and Immunohistochemistry

To generate tissue sections for immunofluorescence and immunohistochemistry, mice were euthanized and perfused via the heart's left ventricle with 10 mL warm PBS followed by 5 mL of 4% paraformaldehyde to fix tissues. To inflate the lung, 2 to 3 mL of a 10% solution of buffered formalin was administered using a 26-g needle inserted into the trachea. Once inflated, the trachea was sealed using a surgical suture. Lungs were then excised and incubated overnight in 10% formalin. Paraffin-embedded sections were primarily used for immunohistochemistry by hematoxylin/eosin, Masson trichrome, and DAB (3,3'-diaminobenzidine) staining. OCT (optimal cutting temperature compound)-embedded sections were prepared by sequential 1-hour incubations in 10%, 15%, and 20% sucrose-PBS and then incubated overnight at 4 °C in a 1:1 solution of 20% sucrose and OCT compound (No. 23730571; Fisher Scientific). The next day, tissues were embedded with OCT compound in cryomolds, and tissue sections (5–10 µm) were collected on an HM525 NX cryotome (Epredia). Tissue sections were dried for 30 minutes at 25 °C, washed 3× in PBS, permeabilized for 20 minutes in 0.2% Triton X-100, and blocked overnight at 4 °C in 10% donkey serum (No. 102644-006; Jackson ImmunoResearch Lab) and 3% BSA-PBS. Antibodies were diluted in 0.02% Triton X-100, 1% BSA-PBS and applied to sections overnight at 4 °C and 3 hours at 25 °C, respectively. For

studies in influenza-infected mice, immunofluorescence was performed using an antibody directed against HA (hemagglutinin) that was obtained through the NIH Biodefense and Emerging Infections Research Resources Repository, NIAID (National Institute of Allergy and Infectious Diseases), NIH: polyclonal anti-influenza virus H1 (H0 [HA], A/Puerto Rico/8/34 [H1N1], antiserum [goat], NR-3148). Images were collected using a Nikon TiE Eclipse epifluorescence microscope or a Nikon C2 confocal microscope and analyzed using the Nikon Elements software (v4). Quantification of expression in immunofluorescence images was performed using ImageJ by normalizing signal intensity against DAPI (4'6-diamidino-2-phenylindole) expression; the operator was blinded to genotype or treatment.

Tissue Permeability Assays

For Evans blue permeability assays, mice were anesthetized by isoflurane inhalation, and 100 to 150 µL of 1% Evans blue (No. E2129; Sigma) that was filtered through a 0.2-µm membrane was administered to mice via the retro-orbital sinus at a final dosage of 40 mg/kg BW. After 1-hour incubation, mice were euthanized and perfused with 10 mL warm PBS. Lung, heart, liver, and kidney tissues were then excised, washed in PBS, and dried overnight at 37 °C. The next day, dry tissue weights were recorded, and 500 µL formamide was added to each sample followed by a 48-hour incubation at 55 °C to extract the Evans blue dye. Samples were briefly centrifuged to remove tissue fragments, and supernatants were used to quantity Evans blue spectrophotometrically (OD_{670} [optical density at 670 nm]) by comparison to a standard curve. Final values were normalized to tissue dry weight. Intravenous injection of FITC (fluorescein isothiocyanate)-dextran (molecular weight [MW], 150 000; FD150S; Millipore Sigma) was similarly performed via the retro-orbital sinus. Mice were administered 100 to 150 µL of a filtered 25 mg/mL FITC-dextran solution at a final dosage of 100 mg/kg BW. FITC-dextran was allowed to circulate for 1 hour, at which time mice were euthanized, perfused with warm PBS, fixed in 4% paraformaldehyde, and then embedded in OCT for tissue sectioning.

Real-Time Quantitative Reverse Transcription PCR

Total RNA was extracted from murine tissue samples or cultured ECs using Trizol and following the manufacturer's instructions. RNA (1 µg) was then converted to cDNA using an iScript cDNA Synthesis Kit (No. 1708891BUN; Bio-Rad), which was then analyzed on a Bio-Rad CFX96 Real-Time Thermocycler using 2X SYBR green qPCR (real-time quantitative reverse transcription PCR) master mix (No. 4312704; Life Technologies). Target gene expression was normalized against 3 reference genes: *Actb*, *Gapdh*, and *Rn18s* (Table S2).

EC Culture and Treatments

Human umbilical vein ECs (HUVECs), isolated as described previously [36] or purchased from commercially available sources (No. PCS-100-010; ATCC [American Type Culture Collection]), were cultured in complete EGM-2 (endothelial growth media-2) media (No. CC-33162; Lonza). For TNFα treatment of HUVECs, cells were treated with 10 ng/mL TNFα (No. 410-MT; R&D Systems) for up to 10 hours followed by the isolation of RNA and protein for qPCR and immunoblot, respectively. For MG132 treatments, HUVECs were treated with 10 µM MG132 (No. BML-PI102; Enzo Life Sciences) or vehicle (DMSO) for 30 minutes before a 6-hour TNFα treatment. Immunoprecipitation of endogenous ERG was performed using HUVECs following MG132/TNFα treatment. Cells were harvested in lysis buffer supplemented with protease and phosphatase inhibitors and the isopeptidase inhibitor N-ethylmaleimide (No. 04259; Sigma). After clarification by centrifugation, 1 mg of total protein cell lysate was incubated with 4 µg of rabbit anti-human-ERG Ab (antibody; No. sc-28680; Santa Cruz) overnight at 4 °C. The immuno-complexes were precipitated with TrueBlot goat-anti-rabbit Ig beads (No. 00-8800-25; Rockland) for 4 hours at 4 °C and detected by western blot with anti-ERG and anti-ubiquitin antibodies.

For siRNA-mediated *Erg* gene knockdown, HUVECs were grown to ≈80% confluence followed by transfection with 100 nM human ERG Silencer Select (No. s4811; Thermo Fisher) or nontargeting siRNA oligos (ERG #4392420 and nontargeting #AM4635; Life Technologies) using lipofectamine RNAiMAX (No. 13778150; Life Technologies) in serum-free OptiMEM (No. 31985070; Life Technologies). Gene knockdown proceeded for 48 hours before cell collection in Trizol for subsequent RNA isolation and qPCR analysis.

Isolation and Cloning of Erg Wild-Type and Mutant Myc-Tagged cDNA

HUVECs were grown on 1% gelatin-coated plates in EGM-2 medium (No. CC3156; Lonza) for 48 hours. Total RNA was extracted using the RNeasy kit (No. 74106; Qiagen). First-strand cDNA synthesis was performed using 1 µg total RNA with superscript III reverse transcriptase (No. 18080093; Invitrogen). PCR amplification was performed with 1 µL cDNA and 0.5 µM Erg001-F forward and Erg-R-Myc reverse primers (Table S2). PCR products were purified using the QIAquick gel extraction kit (No. 28706X4; Qiagen) and ligated into pcDNA3.1 (V79020; Invitrogen). All clones were sequenced from both ends. The pcDNA3.1 ERG (GenBank accession number: NM_182918) Myc-tagged construct was mutated using the QuickChange Lightning Multi Site-Directed Mutagenesis Kit (No. 210513; Agilent). All primers were designed using the QuickChange Primer Design Program (Agilent) and are listed in Table S2. Briefly, pcDNA3.1 ERG Myc-tagged plasmid was amplified using 1 or several primers designed to mutate a specific triplet that codifies from lysine to arginine. All constructs were verified by DNA sequencing. The different mutants generated were as follows: K67R, K89R, K92R, K111R, K271R, K282R, K67-111R, K271-282R, and K67-282R.

For analysis of ubiquitination of transfected ERG, Myc-tagged, HeLa (Henrietta Lacks; human epithelial) cells were transfected with ERG Myc WT (wild-type) or K/R (lysine/arginine) mutants and Flag-tagged ubiquitin (kindly provided by Prof H. Walczak) or empty vectors. Transfection was performed with GeneJuice (No. C134443; Novagen). After 24 hours, cells were pretreated with vehicle (DMSO) or with MG132 for 6 hours. Incubation of cell lysates with polyubiquitin affinity beads (No. 662200-1KIT; Calbiochem) was performed according to the manufacturer's protocol followed by immunoblotting with an anti-ERG Ab (No. sc-353; Santa Cruz).

Analysis of ERG Protein Stability in HeLa Cells

HeLa cells were transfected with ERG Myc WT or ERG Myc K67-282R mutant. After 8 hours, the transfected cells were treated with cycloheximide (C7698; Sigma) at a final concentration of 100 µg/mL for 0, 4, and 6 hours in the presence of MG132 (10 µM; Calbiochem) or DMSO (vehicle). Cells were harvested in lysis buffer supplemented with protease inhibitors, and lysates were subjected to immunoblot analysis to assess the expression level of ERG protein (No. sc-353; Santa Cruz). GAPDH was used as internal control (No. MAB374; Millipore).

Transmission Electron Microscopy

Lung and kidney tissue from *Erg*^{iECko} and control mice were immersion fixed at room temperature in 0.1 M cacodylate buffer (pH 7.5) containing 4% formaldehyde and 2% glutaraldehyde followed by a second fixation in 1% OsO_4. After dehydration, fixed specimens were embedded in epoxy resin. Ultrathin resin sections were stained with solutions containing uranyl acetate and lead acetate and were visualized on an FEI Tecnai G2 transmission electron microscope.

Statistics

The Prism 7.0 software (GraphPad) was used for all statistical assessments. Tests for normality and equal variance were used to determine the appropriate parametric or nonparametric statistical model or to perform data log transformation, if required. The specific test used for each comparison and *P* values are summarized in Table S3. Statistically analyzed data are presented as mean±SD.

Data Availability

The data underlying this article are available in the article and in its Supplemental Material.

RESULTS

TNFα Induces ERG Ubiquitination and Degradation in Cultured ECs

We and others have reported that stimulation of cultured ECs with the proinflammatory cytokine TNFα leads to ERG downregulation in vitro.[20,37] To understand the mechanism of TNFα-induced ERG downregulation, we treated human umbilical vein ECs (HUVECs) with the cytokine and assessed ERG protein and transcript expression by immunoblot and qPCR, respectively. TNFα stimulation led to ERG protein downregulation in HUVECs (Figure 1A), whereas no significant change in *Erg* transcript expression was observed (Figure S1A), suggesting a posttranscriptional mechanism of ERG downregulation, such as regulated protein degradation. In support of this hypothesis, pretreatment of HUVECs with MG312, an inhibitor of the proteasome, prevented TNFα-induced ERG downregulation (Figure 1B; Figure S1B). Since proteins are commonly polyubiquitinated before degradation,[38] we next assessed the ubiquitination status of ERG in HUVECs after TNFα treatment. HUVECs were treated with TNFα in the presence or absence of MG132, and cell lysates were subjected to ERG immunoprecipitation and probed for ubiquitin by immunoblot. TNFα treatment led to the appearance of high-molecular-weight, polyubiquitinated ERG isoforms that increased in abundance following proteasomal inhibition by MG132 (Figure 1C).

Using the ubiquitination site prediction software UbPred, we identified 6 putative ubiquitination sites within ERG: K67, K89, K92, K111, K271, and K282 (Figure 1D). To determine whether any of these sites are ubiquitinated, we transiently transfected HeLa cells with Myc-tagged wild-type ERG or with ERG mutants in which the putative ubiquitinated lysine (K) residues had been mutated to arginine (R; Figure S1C). Treatment of transfected HeLa cells with MG132 for 6 hours led to the accumulation of polyubiquitinated ERG isoforms, which could be further enhanced by cotransfection with a FLAG-tagged ubiquitin construct (Figure S1D). We found that individual mutations of K67R, K271R, and K282R each resulted in a partial reduction in ERG ubiquitination (Figure S1E). However, mutation of all 6 lysine residues (K67-282R) had the most profound effect on ERG ubiquitination (Figure 1E; Figure S1E) and prolonged the half-life of ERG protein following cycloheximide treatment (Figure 1F).

Inflammatory Stimulation Promotes Lung-Specific ERG Downregulation In Vivo

Next, we asked whether TNFα stimulation was similarly capable of driving ERG degradation in vivo. We performed intravenous injections of TNFα into wild-type mice and used immunoblot to assess ERG expression in 2 highly vascularized tissues, the lung and heart. Three hours after challenge, we observed a substantial TNFα-induced downregulation of ERG in the lung but not the heart (Figure 2A and 2B). Moreover, a similar pattern of lung-specific ERG downregulation was observed following treatment with the proinflammatory cytokines IL-1α and IL-1β but not IL-18 (Figure 2A and 2B; Figure S2B).

Pulmonary ECs are particularly prone to activation during systemic inflammatory challenges, such as bacterial sepsis, in which circulating proinflammatory cytokines like TNFα are upregulated. We, therefore, asked whether lung-predominant ERG degradation occurs during a murine model of LPS-induced sepsis. Acute administration of LPS (4 mg/kg BW) to adult wild-type mice resulted in the transcriptional downregulation of *Erg* within the lung, heart, liver, and kidney after 2 hours, while the immune-privileged retina was spared from *Erg* downregulation within this time frame (Figure 2C). However, at 8 hours post-injection, significant LPS-induced downregulation of ERG protein was only observed in the lung by immunoblotting (Figure 2D). This was confirmed by immunostaining for ERG in tissue sections at 8 hours post-LPS challenge, revealing a loss

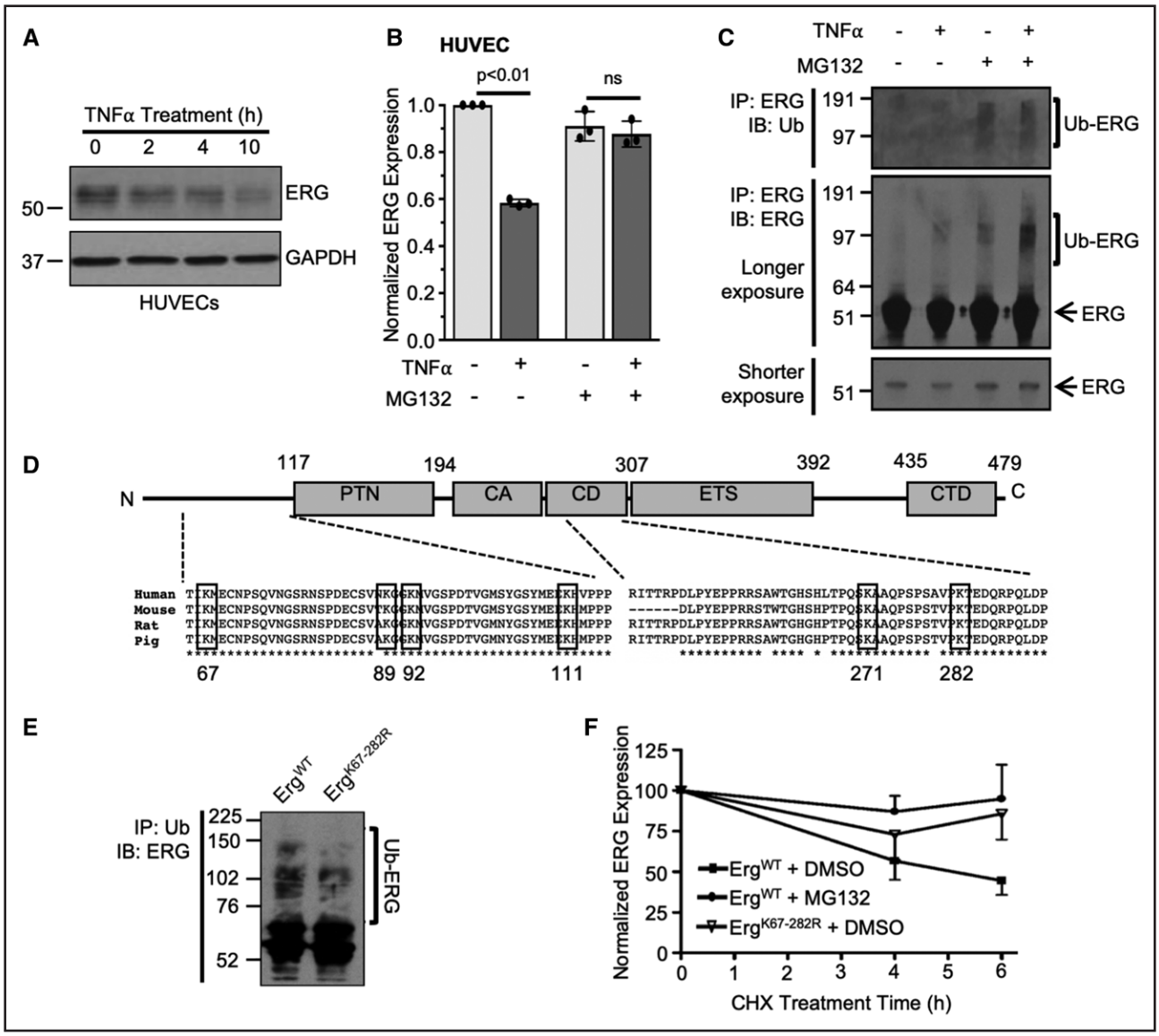

Figure 1. The proinflammatory cytokine TNFα (tumor necrosis factor alpha) promotes ERG (erythroblast transformation-specific–related gene) ubiquitination and proteolytic degradation in vitro.
A, TNFα (10 ng/mL) was applied directly to cultured human umbilical vein endothelial cells (HUVECs), and ERG expression was assessed by immunoblot at the indicated times. **B**, TNFα (10 ng/mL for 6 h)-induced ERG downregulation in HUVECs was assessed by immunoblot (n=3) following a 30-minute pretreatment with MG132 (10 μM). **C**, Following a similar TNFα/MG132 treatment, ERG was immunoprecipitated from HUVECs, and samples were immunoblotted for ERG and ubiquitin (Ub). Longer exposure of the ERG immunoblot revealed the presence of high-molecular-weight, ubiquitinated ERG isoforms. **D**, Alignment of human, mouse, rat, and pig ERG sequences highlighting 6 conserved lysine residues (K) predicted as sites of ubiquitination. **E** and **F**, Mutation of all putative sites to arginine ($Erg^{K67-282R}$) reduced the presence of ubiquitinated ERG isoforms (**E**) and prolonged ERG half-life (**F**) when constructs were expressed in HeLa (Henrietta Lacks; human epithelial) cells (n=3). *P* values were determined by a nonparametric Kruskal-Wallis test followed by a Dunn multiple comparison between the indicated groups. ns indicates nonsignificant.

of ERG expression within $CD31^+$ (cluster of differentiation 31) capillary ECs of the lung (Figure 2E; Figure S2B) that was not observed in the heart, kidney, or liver (Figure S3A through S3D). Furthermore, at this same LPS dose, pulmonary ERG expression began to recover by 24 hours, though we continued to observe a slight but significant reduction in pulmonary ERG expression up to 48 hours post-injection (Figure S2C and S2D). A similar pattern of protein downregulation in the lung following LPS challenge was also observed for the transcription factor FLI1 (Friend leukemia integration 1; Figure S2E), a homologue of ERG with overlapping and compensatory functions.[22,39]

LPS Administration Leads to Cytokine-Induced ERG Degradation in the Lung

We then used genetic models to determine which specific proinflammatory cytokines cause LPS-induced ERG

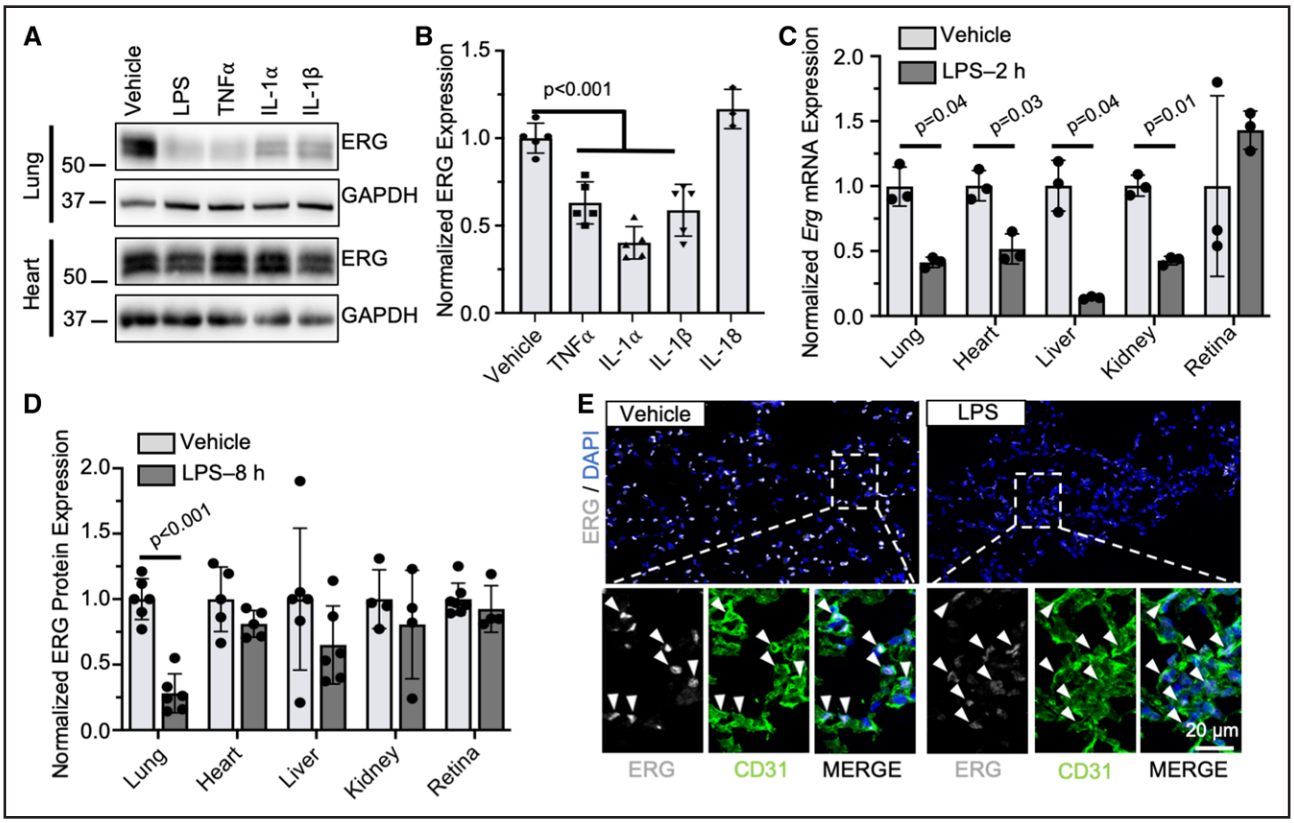

Figure 2. Proinflammatory stimuli promote lung-specific ERG (erythroblast transformation-specific–related gene) protein downregulation.

A and **B**, ERG expression was assessed by immunoblot (**A**) and quantified (n=4–5; **B**) in the lung and heart at 3 hours after intravenous injection of lipopolysaccharide (LPS; 1 mg/kg body weight [BW]), TNFα (tumor necrosis factor alpha), IL (interleukin)-1α, IL-1β, or IL-18 (50 μg/kg BW for each cytokine). **C** and **D**, WT (wild-type) mice were administered intraperitoneal injections of LPS (4 mg/kg BW) or vehicle (0.9% NaCl). *Erg* transcript expression was quantified by qPCR (real-time quantitative reverse transcription polymerase chain reaction) in the indicated organs at 2 hours after LPS exposure (n=3; **C**), and ERG protein expression was quantified by immunoblot at 8 hours after LPS exposure (n=4–6; **D**). **E**, Expression of ERG (gray) in CD31$^+$ (cluster of differentiation 31; green) endothelial cells (white arrows) within the lung was assessed by immunostaining tissue sections collected 8 hours after LPS exposure. DAPI (4',6-diamidino-2-phenylindole; blue) was used as a nuclear counterstain. *P* values were determined by a 1-way ANOVA followed by a Dunnett comparison of each treatment to the vehicle-treated condition (**B**), unpaired *t* tests with Welch correction comparing vehicle- and LPS-treated samples within each organ (**C**), or unpaired *t* tests comparing vehicle- and LPS-treated samples within each organ (**D**).

downregulation in the lung. When we administered LPS (4 mg/kg BW) to mice in which the *TNFα* gene was globally deleted (*Tnfa*$^{-/-}$), we saw a significant rescue of the LPS-induced pulmonary ERG downregulation seen in littermate control mice (Figure 3A). Global deletion of the primary receptor for IL-1α/β (*Il1r1*$^{flox/flox}$*;Sox2-Cre*$^+$*=Il1r1*^{Gko}) was also sufficient to prevent LPS-induced downregulation of pulmonary ERG (Figure 3B). However, deletion of *Il1r1* specifically from ECs using 2 independent Cre lines failed to rescue LPS-induced ERG downregulation in the lung (Figure 3C; Figure S2F), suggesting that IL-1α/β likely works through an intermediate cell type to stimulate pulmonary endothelial ERG downregulation. In agreement with this, adding either IL-1α or IL-1β to TNFα did not affect ERG downregulation in HUVECs (Figure S2G).

We next monitored the kinetics of pulmonary ERG downregulation following acute LPS (10 mg/kg BW) challenge. LPS-induced ERG protein downregulation in the lung was rapid: within 1 hour of LPS administration, we observed a >70% reduction in ERG protein expression (Figure 3D). In contrast, cardiac ERG protein expression was unaffected by LPS challenge during this time frame and only began to trend downward by 24 hours post-LPS challenge (Figure 3E). Interestingly, we observed LPS-induced transcriptional downregulation of *Erg* in both the lung and heart. However, transcriptional downregulation of *Erg* in the lung lagged behind the downregulation of ERG protein (Figure 3D), which is consistent with LPS-induced ERG degradation in vivo similar to what was observed for HUVECs in vitro (Figure 1B). In support of this hypothesis, pretreatment of wild-type mice with MG132 partially prevented LPS-induced ERG downregulation in the lung (Figure 3F).

These data suggest a lung-specific mechanism of cytokine-induced ERG ubiquitination and degradation.

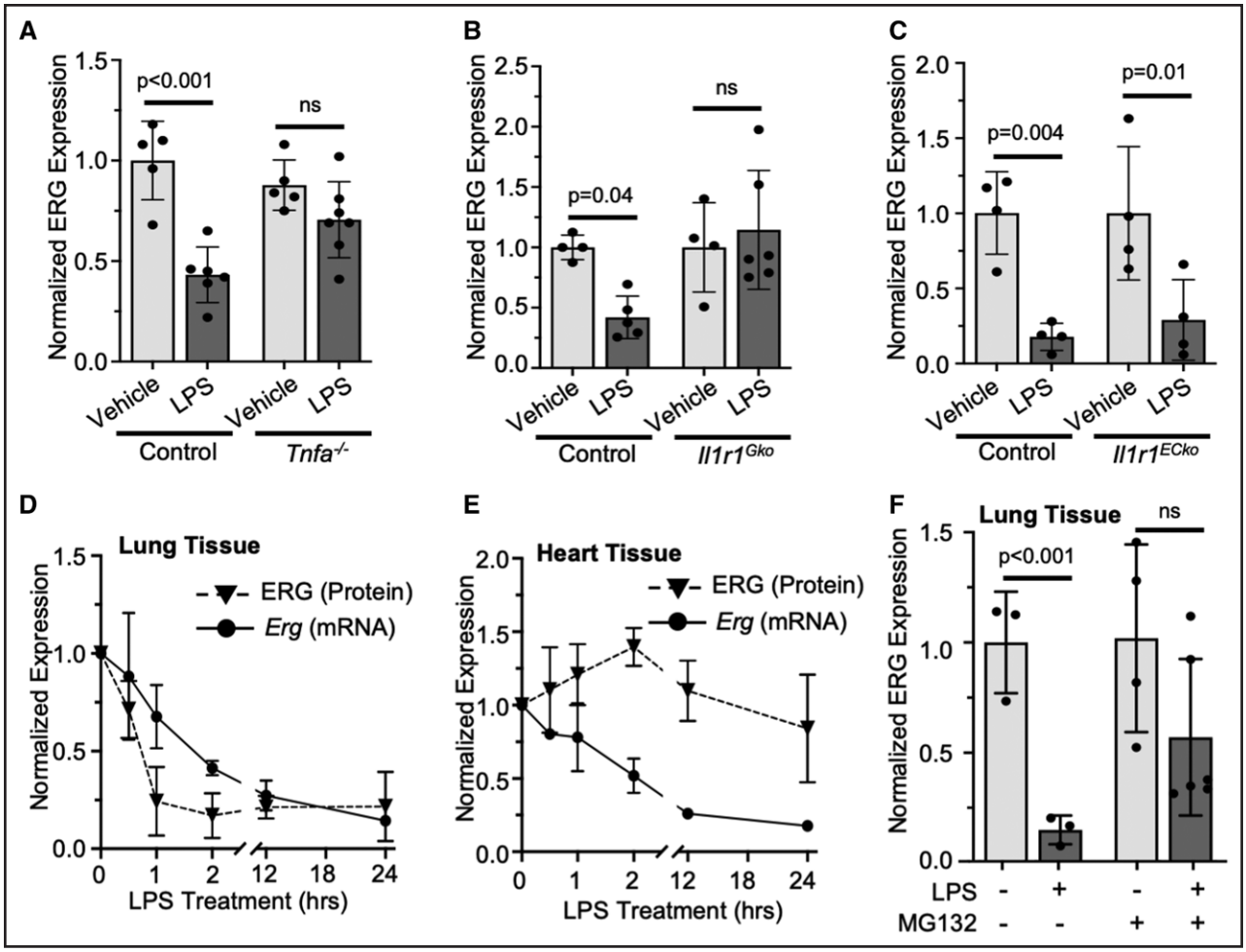

Figure 3. Proinflammatory cytokines promote lipopolysaccharide (LPS)-induced ERG (erythroblast transformation-specific–related gene) degradation in the lung.

A through **C**, ERG expression was assessed by immunoblotting lung lysates at 4 hours after intraperitoneal administration of LPS (4 mg/kg body weight [BW]) in mice following global deletion of *Tnfa* (*Tnfa*$^{-/-}$; n=5–6; **A**), global deletion of *Il1r1* (*Il1r1*^{Gko}; n=4–5; **B**), or endothelial cell–specific deletion of *Il1r1* (*Il1r1*^{ECko}; n=5; **C**). **D** and **E**, Wild-type mice were given an intraperitoneal injection of LPS (10 mg/kg BW). At 0.5 to 24 hours after LPS challenge, ERG protein and transcript expression were quantified in lung (**D**) and heart (**E**) tissues by immunoblot and qPCR (real-time quantitative reverse transcription polymerase chain reaction), respectively (n=3–4). **F**, LPS (4 mg/kg BW)-induced ERG downregulation in the lung was assessed by immunoblot following a 3-hour pretreatment with vehicle or MG132 (10 mg/kg BW; n=3–6). *P* values were determined by a 2-way ANOVA followed by a Sidak multiple comparison test; data that failed a Spearman equal variance test were log transformed before analysis (**B**, **C**, and **F**). ns indicates nonsignificant.

We, therefore, asked whether lung ECs might uniquely express a ubiquitin ligase that targets ERG for degradation. We took advantage a recently published list of EC-expressed gene transcripts within the lung, heart, liver, and kidney that was assembled using translating ribosome affinity purification.[40] This list was cross referenced against a comprehensive database of mammalian ubiquitin ligase genes[41] to generate a list of ≈280 ubiquitin ligases expressed within ECs of each organ (Table S1). Included in this list were previously identified regulators of ERG ubiquitination such as *Trim25*, which impacts ERG degradation in ECs, and *Spop*, which can degrade ERG in prostate cancer cells.[25,42,43] Notably, *Trim25* was ≈2-fold more abundant in lung ECs relative to ECs of the kidney and liver, although lung and heart ECs had more comparable levels of *Trim25* expression (Table S1). Moreover, for an additional ≈30 ubiquitin ligase genes, we observed >2-fold higher expression in lung ECs compared with the ECs from any other organ (Table S1). However, future studies will be needed to determine whether expression of these ubiquitin ligases plays a role in lung-specific ERG degradation.

ERG Is Downregulated in Pulmonary ECs After an Influenza Challenge

Since proinflammatory cytokines, such as TNFα, are also produced in the lung during viral infections, we determined whether pulmonary ECs downregulate

ERG during a murine model of influenza infection.[44] We assessed ERG expression following intratracheal exposure to a mouse-adapted influenza virus and observed a significant decrease in ERG protein expression 6 days after administration of low (800 egg infectious dose) and high (1050 egg infectious dose) viral doses (Figure 4A). Immunostaining of influenza-infected lungs revealed reduced ERG expression relative to the lungs of vehicle-injected mice (Figure 4B; Figure S4). Intriguingly, ERG downregulation was more substantial in pulmonary capillary beds relative to larger caliber blood vessels, which appeared to maintain higher ERG expression (Figure 4B; Figure S4). In addition, the influenza virus was regionally localized within infected lungs, as evidenced by immunostaining for the influenza protein HA (Figure 4C). Importantly, immunostaining of influenza-infected lungs revealed a loss of ERG expression that colocalized with the heavily infected (HA positive) regions of the lung (Figure 4C).

Transcriptional Regulation of *Tek*/TIE2 by ERG in Pulmonary ECs In Vivo

ERG is a master regulator of endothelial gene expression[19,45]; thus, the downregulation of ERG during a systemic inflammatory challenge likely has a substantial impact on pulmonary resilience of ECs in the inflamed lung. One of the key mediators of lung vascular homeostasis regulated by ERG is TIE2 (tunica interna endothelial cell kinase 2; gene name, *TEK*),[18,23] an EC-expressed receptor tyrosine kinase that maintains vascular stability under homeostatic conditions.[46] The connection between *TEK*/TIE2 repression and pulmonary vascular dysfunction in sepsis/ARDS is well documented.[47–51]

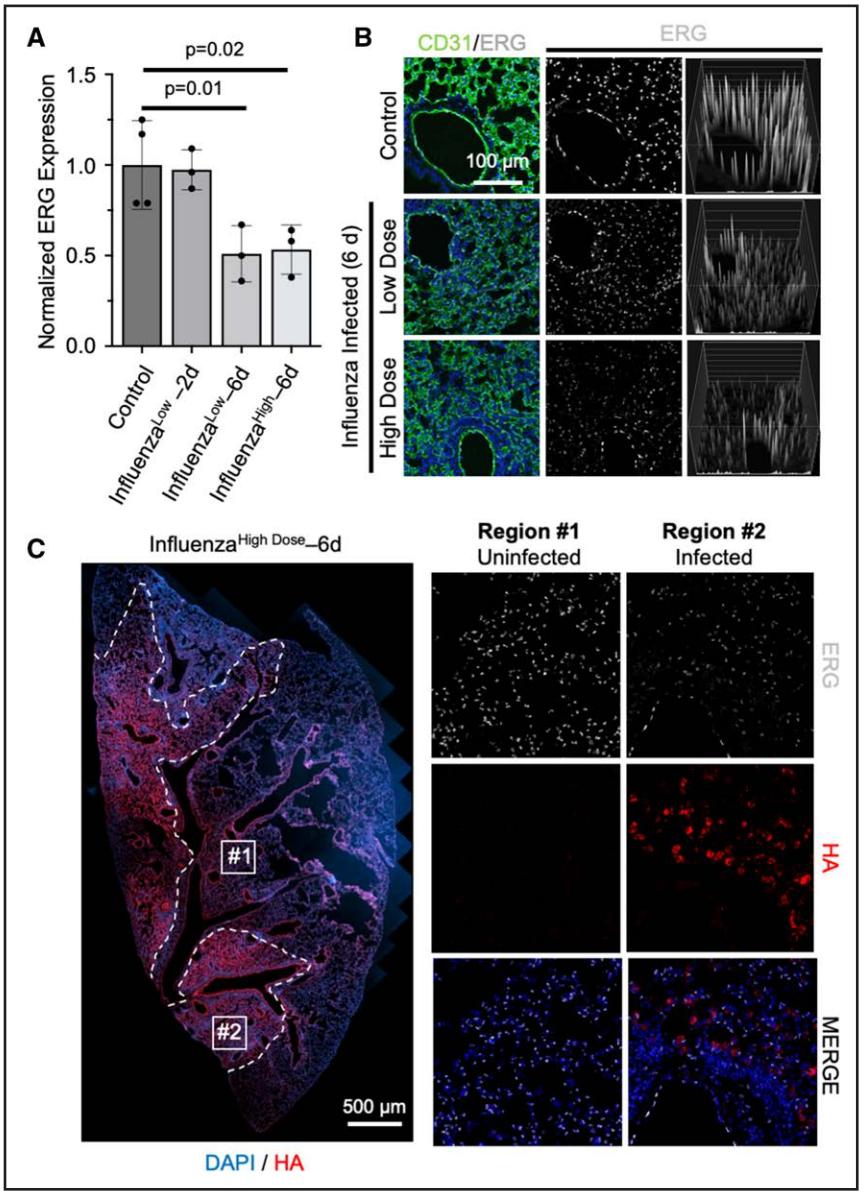

Figure 4. ERG (erythroblast transformation-specific–related gene) is downregulated in the lung during pulmonary influenza infection.
A, ERG expression was quantified by immunoblot using murine lung tissue collected 2 and 6 days after low (800 egg infective dose [EID]) and high (1050 EID) doses of influenza were administered via the trachea (n=3). **B**, Expression of ERG (gray) in endothelial cells (ECs; CD31 [cluster of differentiation 31]; green) was assessed by immunostaining lung tissue sections collected from control or influenza-infected mice. Reduced ERG expression within pulmonary capillary ECs (but not within ECs of larger caliber vessels) of influenza-infected mice is visualized by a surface intensity representation of the ERG channel (**right**); DAPI (4',6-diamidino-2-phenylindole; blue) was used as a nuclear counterstain. **C**, Immunostaining for the influenza HA (hemagglutinin) protein (red) was used to identify uninfected (No. 1) and infected (No. 2) regions of a lung section. Reduced expression of ERG (gray) was observed in infected regions relative to uninfected regions of the same lung section. *P* values were determined by a 1-way ANOVA followed by a Dunnett multiple comparison test.

During inflammation, multiple pathways contribute to the repression of TIE2 expression and activity, resulting in pulmonary blood vessel destabilization.[52] However, little is known regarding the mechanisms of transcriptional *TEK* repression in the inflamed lung.

In agreement with our previous work,[18] siRNA-mediated *ERG* knockdown in HUVECs led to a downregulation of *TEK* transcript expression (Figure 5A). We, therefore, used HUVECs to investigate the molecular mechanisms through which ERG regulates *TEK* expression. Analysis of ERG binding to DNA in HUVECs via chromatin immunoprecipitation sequencing[45] identified an ERG-binding peak associated with an intronic region mapped to the *TEK* gene locus, downstream of the transcription start site (Figure 5B). The site was also enriched for the histone modification H3K27Ac and for RNAPol2 (RNA polymerase II), suggesting the presence of an active enhancer region. Chromatin immunoprecipitation followed by qPCR confirmed ERG enrichment at the *TEK* intronic region (Figure 5C).

To investigate whether ERG regulates the expression of *Tek*/TIE2 in vivo, we genetically deleted *Erg* from ECs using a tamoxifen-inducible EC-specific Cre[28] (Figure S5A) and a floxed allele of *Erg* (*Erg*$^{fl/fl}$*;Cdh5[PAC]-CreERT2*=*Erg*^{iECko}), and we used qPCR to quantify *Tek* transcripts in the lung, heart, liver, and kidney. Surprisingly, we observed significant *Tek* downregulation in the lungs of *Erg*^{iECko} mice but not in the other organs tested (Figure 5D). A similar pattern was observed for TIE2 protein, which was significantly downregulated in the lungs of *Erg*^{iECko} mice but not the heart, liver, or kidney (Figure 5E and 5F). These findings were further supported by immunostaining for TIE2 in lung sections collected from *Erg*^{iECko} mice, which revealed a substantial loss of TIE2 expression within CD31^{+} capillary ECs (Figure 5G; Figure S6A). Therefore, ERG regulates *Tek* expression in vivo in an organotypic manner.

To determine whether *Tek* is also regulated in an organotypic manner during a systemic state of inflammation, we performed intraperitoneal LPS injections in wild-type mice and used qPCR to assess *Tek* expression in the lung and heart at 6 to 72 hours after LPS challenge. In both tissues, we observed a maximum *Tek* downregulation (>80%) at 6 hours post-LPS injection. However, in the lung, the downregulation of *Tek* expression persisted for up to 72 hours, whereas in the heart, *Tek* expression had recovered to a basal level by 24 to 48 hours post-LPS injection (Figure 5H and 5I). Thus, *Tek* regulation after an LPS challenge in vivo in the lung vasculature mirrors that of ERG protein expression.

We and others have previously shown that ERG controls vascular stability and barrier integrity through additional targets besides *TEK*.[19,45,53,54] We, therefore, assessed the impact of ERG expression on *Cdh5* and *Cldn5*, components of EC adherens and tight junctions, respectively, which were previously identified as transcriptional targets of ERG.[21,36] In agreement with previous work, silencing of *ERG* in HUVECs led to the transcriptional downregulation of both *CDH5* and *CLDN5* (Figure S6B). However, the expression of neither gene was affected in the lungs of *Erg*^{iECko} mice (Figure S6C), suggesting that an in vivo context impacts ERG activity. Notably, *Cdh5* and *Cldn5* were likewise not downregulated in the lungs of wild-type mice at 6 or 24 hours after LPS challenge, although *Tek* was downregulated at both these time points (Figure S6D).

EC-Specific Deletion of *Erg* Leads to Pulmonary Vascular Hyperpermeability and Immune Cell Infiltration

We next turned our attention to understanding how the loss of ERG expression in pulmonary ECs might contribute to well-known features of the inflamed lung. First, we determined the impact of ERG downregulation on vascular permeability by performing an Evans blue dye leakage assay in *Erg*^{iECko} and littermate control mice. In agreement with a recent study,[23] lungs from *Erg*^{iECko} mice displayed increased pulmonary vascular permeability compared with those from control mice using fluorometric quantification of extravasated dye (Figure 6A). However, we also noticed that ERG-dependent vascular hyperpermeability was more prominent in the lung when compared with the other organs tested. We, therefore, used an alternative measure of vascular permeability by performing intravenous injection of FITC-dextran (MW, 150 000), which is too large to exit from most nonactivated blood vessels. After 1 hour, mice were perfused to remove vascular FITC-dextran, and lung, heart, liver, and kidney tissues were collected for analysis by immunostaining. We observed substantially more extravascular FITC-dextran in the lungs of *Erg*^{iECko} mice compared with control mice, indicative of vascular hyperpermeability in the mutants (Figure 6B). In agreement with our Evans blue dye assay, deletion of endothelial *Erg* had a less dramatic effect on permeability in other organs (Figure 6C).

ERG has been shown to regulate the expression of EC-expressed leukocyte adhesion molecules such as *Icam1* and *Vcam1* in vitro and in vivo.[54] We, therefore, used immunoblots to assess pulmonary ICAM1 (intercellular adhesion molecule 1) and VCAM1 (vascular cell adhesion molecule 1) expression following the deletion of endothelial *Erg*. We detected a significant upregulation of VCAM1, but not ICAM1, in the lungs of *Erg*^{iECko} mice compared with control littermates (Figure 6D through 6F). Although immune cell recruitment occurs at the postcapillary venules within most organs, the lung is unique in that this process is largely restricted to capillary ECs.[55] Consistently, immunofluorescence imaging of control and *Erg*^{iECko} lung tissue sections revealed that VCAM1 was most prominently upregulated within the pulmonary capillary bed (Figure 6G).

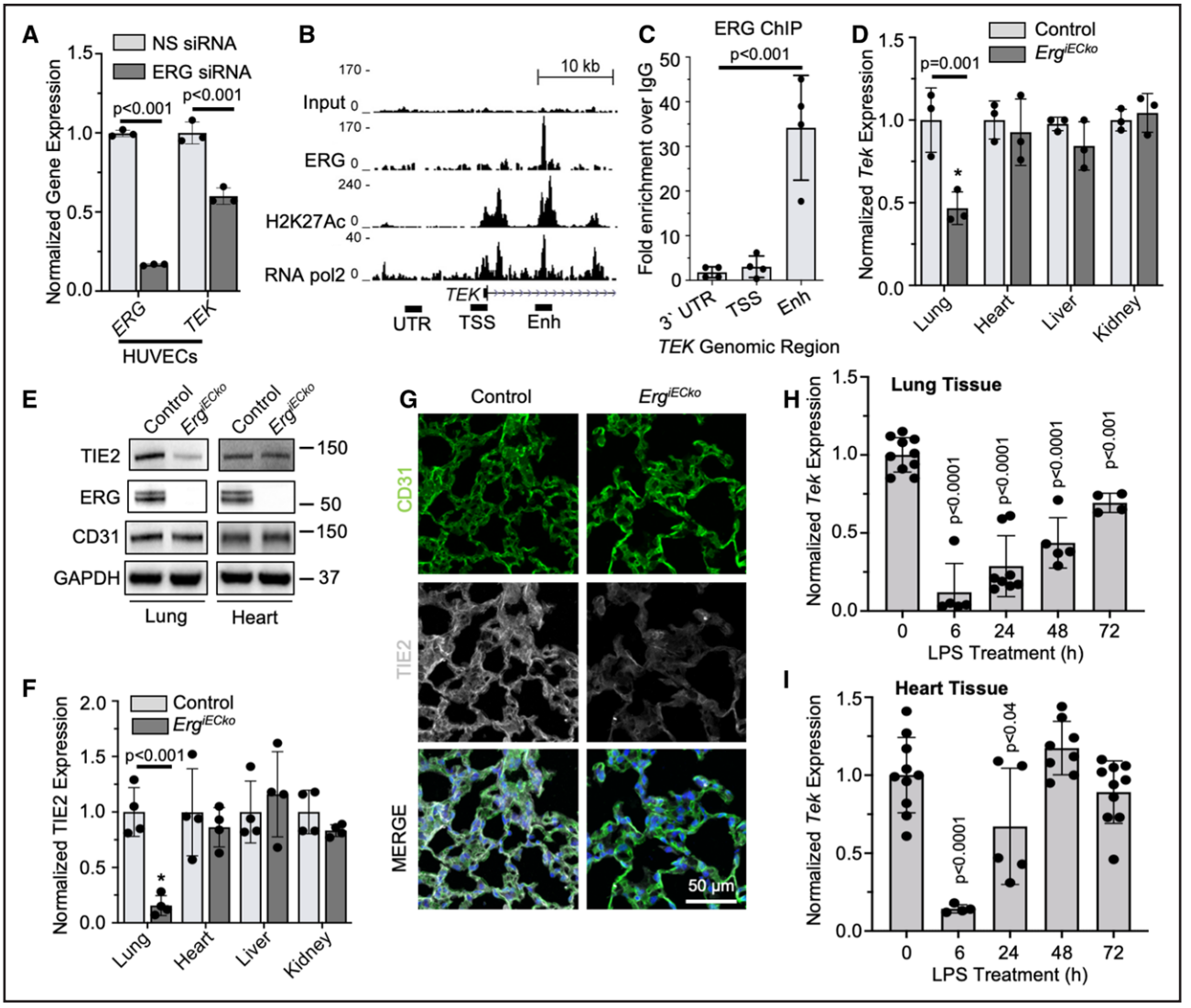

Figure 5. Tek is transcriptionally regulated by ERG (erythroblast transformation-specific–related gene).
A, *TEK* and *ERG* expression in human umbilical vein endothelial cells (HUVECs) was assessed by qPCR (real-time quantitative reverse transcription polymerase chain reaction) following siRNA-mediated *ERG* knockdown (n=3). **B** and **C**, ERG chromatin immunoprecipitation (ChIP) sequencing (**B**) identified occupancy of ERG at the *TEK* transcriptional start site (TSS) and an intragenic region that colocalizes with H3K27Ac, a marker of active enhancers, in HUVECs. ERG binding to the TSS, an enhancer region, was confirmed by ChIP-qPCR (**C**; n=4). **D**, *Tek* transcript expression was assessed by qPCR in the lung, heart, liver, and kidney of *Erg*^{iECko} and control littermates (n=3). **E** and **F**, TIE2 (tunica interna endothelial cell kinase 2) protein expression in *Erg*^{iECko} and control littermates was assessed by immunoblot (**E**) and quantified (n=4) in the lung, heart, liver, and kidney (**F**). **G**, Expression of TIE2 (gray) in CD31^{+} (cluster of differentiation 31; green) endothelial cells in the lungs of control and *Erg*^{iECko} mice was assessed by immunofluorescence. DAPI (4'6-diamidino-2-phenylindole; blue) was used as a nuclear counterstain. **H** and **I**, *Tek* expression was assessed by qPCR in WT (wild-type) murine lung (**H**) and heart (**I**) tissues collected 6 to 72 hours after lipopolysaccharide (LPS; 4 mg/kg body weight [BW]) challenge (n=5–7). **A**, **D**, and **F**, *P* values were determined by unpaired *t* tests comparing NS and ERG siRNA-treated groups (**A**) or between control and *Erg*^{iECko} animals within each organ (**D** and **F**). **C**, **H**, and **I**, *P* values were determined by 1-way ANOVA followed by Dunnett multiple comparison tests.

During inflammation, vascular hyperpermeability and adhesion molecule expression collectively facilitate the recruitment and extravasation of immune cells into the lung and other tissues.[56,57] Moreover, ERG inhibition has been shown to promote immune cell recruitment in vitro and in vivo.[20,23] We, therefore, assessed the abundance of immune cells in the lungs of *Erg*^{iECko} and control mice using the pan-immune cell marker CD45,[58] revealing greater numbers of CD45^{+} cells in the lungs of *Erg*^{iECko} mice (Figure 6H and 6I). Importantly, a similar increase in pulmonary immune cells was also observed using an independently generated *Erg*^{iECko} line (Figure S5B). Neutrophils are among the first immune cells recruited to the inflamed lung.[59–61] In agreement with others,[23] we observed a greater number of MPO (myeloperoxidase)-positive neutrophils in the lungs of *Erg*^{iECko} mice (Figure 6H and 6J). In contrast, *Erg* depletion had no apparent effect on the

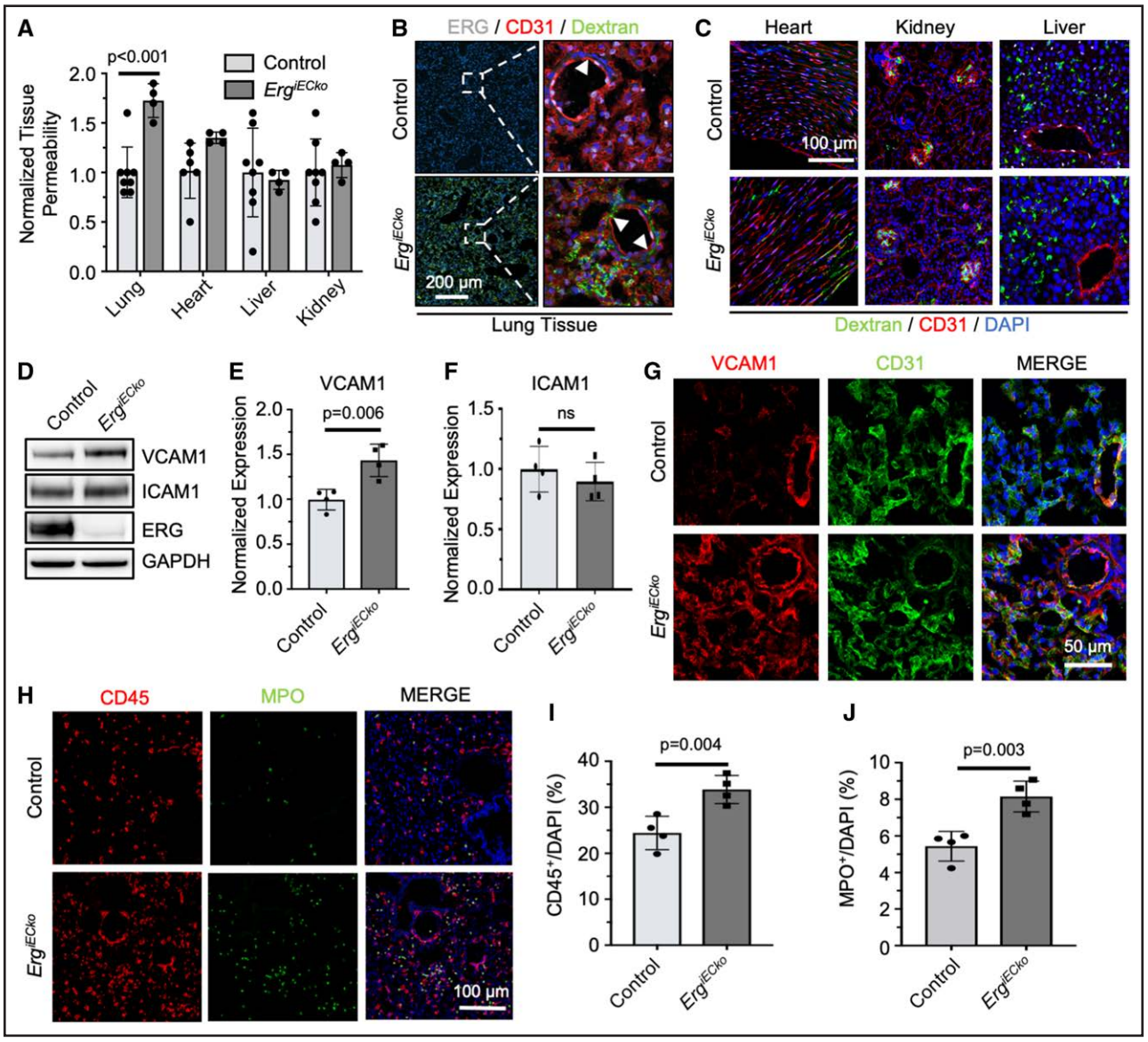

Figure 6. Vascular permeability, adhesion molecule expression, and immune cell recruitment occur in the lungs of *Erg*^{iECko} mice. **A**, Evans blue dye leakage in the lung, heart, liver, and kidney from control and *Erg*^{iECko} mice was spectrophotometrically quantified and normalized to dry tissue weight (n=4–6). **B** and **C**, Intravenously injected FITC (fluorescein isothiocyanate)-Dextran (green; molecular weight [MW], 150 000 kDa) could be visualized outside of pulmonary blood vessels (CD31 [cluster of differentiation 31]; red; white arrows) in *Erg*^{iECko} mice but not in littermate controls (**B**). However, extravasation of FITC-Dextran in the heart, liver, and kidney following endothelial *Erg* (erythroblast transformation-specific–related gene) deletion was less apparent (**C**) ERG (gray); DAPI (4'6-diamidino-2-phenylindole; blue). **D** through **G**, Elevated expression of VCAM1 (vascular cell adhesion molecule 1), but not ICAM1 (intercellular adhesion molecule 1), in the lungs of *Erg*^{iECko} mice was detected by immunoblot (**D**) and quantified (**E**–**F**; n=4). VCAM1 upregulation, particularly in the capillary bed of *Erg*^{iECko} lungs, was confirmed by immunofluorescence imaging (**G**). **H** through **J**, Greater numbers of CD45$^+$ (red) immune cells and MPO$^+$ (myeloperoxidase; green) neutrophils were observed in the lungs of *Erg*^{iECko} mice relative to their control littermates (**H**), which was quantified by normalization against nuclei (DAPI; blue; **I** and **J**). *P* values were determined by unpaired *t* tests comparing control and *Erg*^{iECko} experimental groups. ns indicates nonsignificant.

numbers of MPO$^+$ immune cells in the heart, liver, or kidney (Figure S5C through S5E).

EC-Specific Deletion of *Erg* Leads to Organotypic Tissue Fibrosis and Disrupts Pulmonary Vascular Structure

Although vascular hyperpermeability and immune cell recruitment play beneficial roles in acute inflammatory responses, prolonged inflammation and vascular instability can lead to tissue fibrosis. We, therefore, used a Masson trichrome stain to assess collagen deposition in the lung, liver, heart, and kidney of control and *Erg*^{iECko} mice. Deletion of *Erg* resulted in a substantial increase in collagen deposition in the lung, accompanied by significant structural disruptions; the liver and heart also showed increased collagen deposition in *Erg*^{iECko} mice, albeit to a lesser extent, while no major difference was

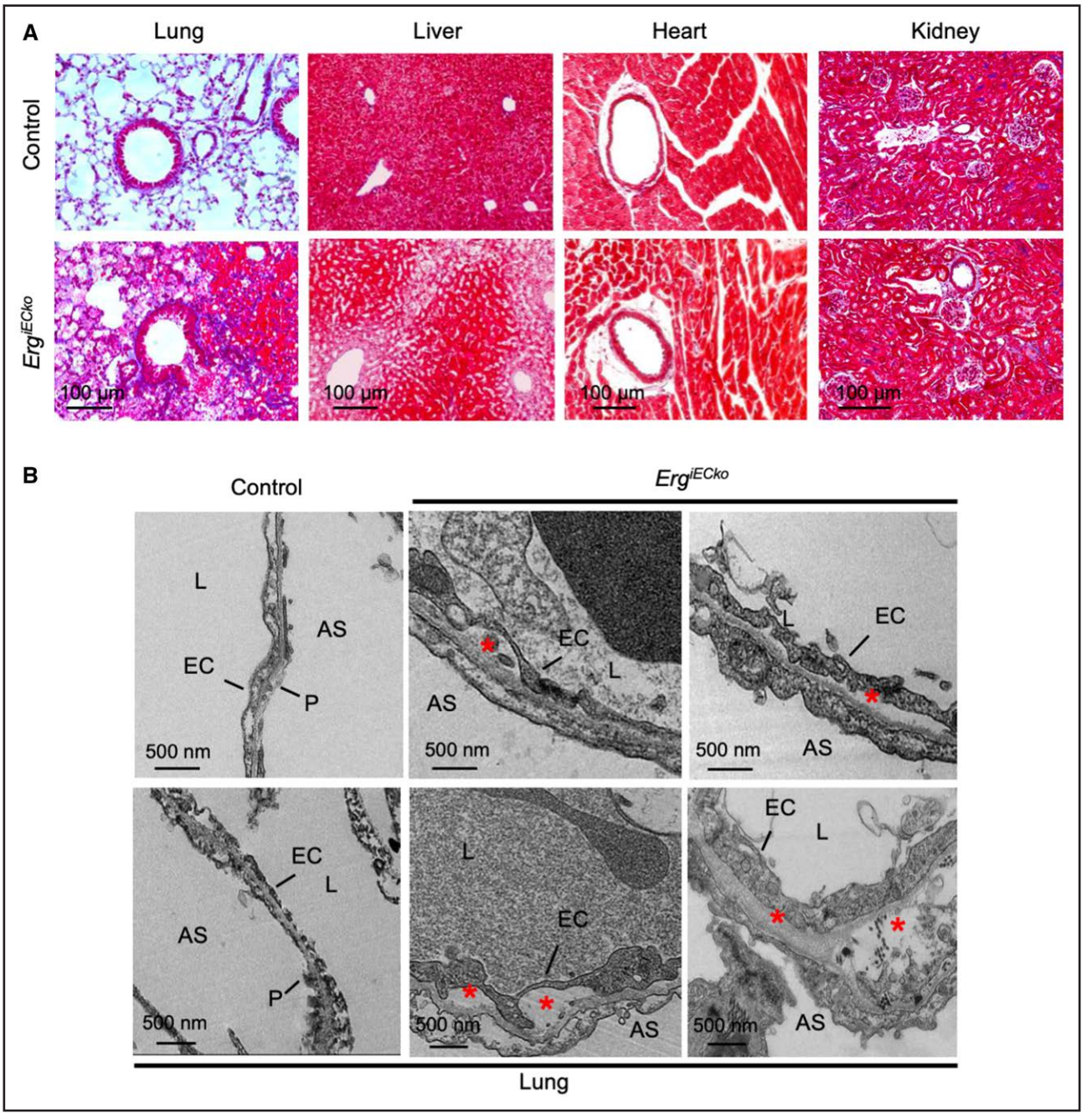

Figure 7. Deletion of endothelial *Erg* (erythroblast transformation-specific–related gene) leads to organotypic fibrosis and disruption of vascular structures within the lung.

A, Masson trichrome staining was used to assess collagen (blue) deposition within the lung, liver, heart, and kidney of *Erg*^{iECko} and control mice. **B** and **C**, Transmission electron microscopy was used to assess microvascular structures within the lung (**B**) and kidney (**C**) from *Erg*^{iECko} and control mice. In the lung, deletion of endothelial *Erg* led to endothelial cell (EC) hypertrophy and basement membrane delamination (red asterisks) resulting in a separation from pneumocytes (P) and the enlargement of the membrane separating alveolar air sacs (AS) and vascular lumens (L).

found for the kidney (Figure 7A). We, therefore, used transmission electron microscopy to explore the consequences of *Erg* deletion on lung microvascular structures. In lungs from control mice, ECs and pneumocytes form thin layers that separate the blood from alveolar air sacs. However, these structures were dramatically disrupted in *Erg*^{iECko} mice. We observed signs of EC hypertrophy and basement membrane delamination that led to a pronounced thickening of the membrane separating the blood and alveolar compartments (Figure 7B). Thus, our data indicate that despite its ubiquitous expression in ECs, the loss of ERG has organotypic functional and structural consequences that are most evident in the lung microvasculature.

DISCUSSION

Each year, sepsis affects ≈20 million individuals worldwide with mortality rates among hospitalized patients ranging from 17% to 26%.[62] The progression of sepsis is complex, resulting from the collective disruption of multiple organ systems by a rampant proinflammatory response to blood-borne bacterial infection. However, impaired respiratory function is one of the most common manifestations of sepsis.[63] In 6% to 7% of patients, continued deterioration of pulmonary function results in ARDS for which mortality rates can be as high as 40%.[64,65] Within these patients, inflammation-induced destabilization of pulmonary blood vessels disrupts fluid homeostasis and impairs efficient gas exchange between the blood and alveolar air sacs thereby undermining organ function.[66] In addition to sepsis, ARDS can result from seemingly diverse conditions including viral/fungal infection,[67,68] burn injury,[69] brain injury,[70] drug overdose,[71] or pancreatitis,[72] suggesting that the lung may be generally prone to vascular dysfunction under inflammatory challenge. Yet the mechanistic reasons for this predisposition are poorly understood. As a result, we currently lack therapeutic options that effectively target the pathogenesis of vascular dysfunction within the lungs of sepsis/ARDS patients.[66]

Here we have demonstrated how organotypic regulation of the master endothelial transcription factor ERG preferentially destabilizes pulmonary blood vessels during a systemic inflammatory challenge. Acute LPS exposure led to the downregulation of *Erg* mRNA transcripts in the lung, heart, liver, and kidney; yet the rapid downregulation of ERG protein was only observed in the lung. We speculate that these are independent processes collectively resulting in a more rapid and substantial loss of ERG protein in the lung when compared with other organs. ERG proteolysis has primarily been studied in the context of cancerous prostate epithelial cells, in which oncogenic ERG fusion proteins evade recognition by the SPOP (speckle-type POZ [pox virus and zinc finger protein] protein) and TRIM25 (tripartite motif 25) ubiquitin ligases[73,74]; 2 recent studies have also documented ERG degradation in cultured ECs.[24,25] The identity of the ubiquitin ligase responsible for lung-specific ERG degradation is an important question that is ultimately unaddressed by this study. However, using a previously published data set,[40] we have generated a list of ubiquitin ligase genes expressed by ECs from multiple organs to ask whether lung ECs harbor unique proteolytic machinery that may target ERG for ubiquitination/degradation (Table S1). Notably, this list confirms that the known ERG ubiquitin ligases TRIM25 and SPOP are expressed by pulmonary ECs. However, the expression of neither gene was confined to lung ECs, raising the possibility that lung-specific ERG degradation results from the selective activation or regulation of a widely expressed ubiquitin ligase. We also identified ≈30 ubiquitin ligases that were >2-fold higher expressed in lung ECs compared with other organs. Included in the list is TRIM8, an additional member of the TRIM family of ubiquitin ligases that was ≈4-fold more highly expressed in lung ECs compared with the other organs. TRIM8 inhibition alleviates LPS-induced lung inflammation.[75] Moreover, TRIM8 mediates the ubiquitination/degradation of the ERG homologue FLI1 in cancerous prostate epithelial cells.[76] However, TRIM8 has not yet been studied in the context of ECs and is, therefore, an interesting candidate for future studies.

The transcriptional responses of activated ECs vary across vascular beds.[40,77] Therefore, lung-specific degradation of ERG, which has well-documented anti-inflammatory and prohomeostatic functions, likely contributes to organotypic transcriptional responses of pulmonary ECs.[19] Indeed, loss of endothelial *Erg* expression has a substantial effect on pulmonary vascular function, as recently demonstrated in a murine model of the aging lung.[23] In agreement with that study, we found that inducible genetic deletion of endothelial *Erg* is sufficient to drive pulmonary vascular permeability, immune cell recruitment, and fibrosis. This study brings new information to light by demonstrating that these effects were more dramatic in the lung despite the deletion of *Erg* in all ECs, highlighting the importance of in vivo context for ERG function. We and others have proposed that context-specific activities of a pan-endothelial transcription factor like ERG are influenced by organotypic transcription factors.[78] Therefore, we speculate that lung-specific ERG functions are impacted by local factors in pulmonary ECs.

The severity of phenotype observed in the lungs of Erg^{iECko} mice suggests that the loss of endothelial *Erg* expression has a substantial impact on EC gene expression. In this study, we chose to focus on the regulation of *Tek*, since reduced expression of *Tek*/TIE2 plays a causal role in the destabilization of pulmonary blood vessels during sepsis/ARDS.[47,49] Under basal conditions, *Tek*/TIE2 is highly expressed by ECs and promotes vascular stability and quiescence through downstream AKT signaling and inhibition of the transcriptional activity of FOXO1 (forkhead box protein O1).[48,50] Under inflammatory challenge, multiple pathways converge on the inhibition of TIE2 activity, thereby relieving FOXO1 inhibition to initiate proinflammatory responses. Our data indicate that following acute LPS challenge, *Tek* expression in the lung and heart is initially downregulated to a similar extent, yet basal *Tek* expression was restored more slowly in the lung. Interestingly, the recovery of *Tek* transcripts coincided with the recovery of ERG protein expression following acute LPS challenge. Therefore, we speculate that within the inflamed lung, the loss of ERG expression impairs the recovery of *Tek* expression following its downregulation during the acute phase of inflammation. Importantly, ERG regulates many additional genes that influence the vascular inflammatory response.[20,21,37,53,54,79] Therefore, it will be interesting to determine whether

these genes are likewise regulated by ERG in an organotypic and stimulus-specific manner.

Constitutive deletion of *Erg*, which is highly expressed by nearly all ECs, causes embryonic lethality between days 10.5 and 11.5.[32] Postnatal downregulation of endothelial ERG is associated with multiple organ phenotypes, including tissue fibrosis,[23,80] bleeding and thrombosis,[79] and ocular vascular regression[78] via the regulation of critically important pathways such as Wnt/β-catenin,[32] TGFβ,[80] KLF-2 (Krüppel-like factor 2),[79] and angiopoietin signaling.[18] Accordingly, loss of ERG expression in human diseases is associated with atherosclerosis,[54] liver fibrosis,[80] and pulmonary hypertension.[22] For these reasons, ERG has been identified as a critical mediator of vascular function.[19] ERG is frequently coexpressed in ECs along with its homologue FLI1, with which it shares ≈75% sequence similarity. ERG and FLI1 exhibit overlapping and often compensatory functions,[22,81,82] and we recently demonstrated loss of vascular identity and systemic vascular collapse following the inducible endothelial deletion of both *Erg* and *Fli1* in adult mice.[39] Therefore, our observation that both ERG and FLI1 are rapidly downregulated in the lungs of LPS-challenged mice suggests a common mechanism to their degradation and raises questions about their combinatorial impact on the response to vascular inflammation in pulmonary ECs.

Altogether, this study adds to our growing appreciation of EC heterogeneity by providing new insights into the organotypic vascular response to inflammation. Our work indicates that the widely expressed endothelial transcription factor ERG, a master regulator of endothelial function, is targeted by cytokines for preferential proteolytic degradation in the lung. Based on our data, we propose that during inflammation, acute ERG downregulation helps coordinate a transcriptional response within pulmonary ECs to support vascular hyperpermeability and immune cell recruitment. However, sustained loss of endothelial ERG impairs the ability of the lung to return to homeostasis, thereby predisposing the lung to vascular dysfunction. Therefore, identification of the mechanism by which inflammatory cytokines trigger pulmonary ERG degradation could yield new therapeutic targets for combating lung-damaging diseases such as sepsis and ARDS.

ARTICLE INFORMATION

Received January 3, 2023; accepted May 31, 2023.

Affiliations

Cardiovascular Biology Research Program (C.M.S., K.K., M.-L.W., C.F.J., A.B., E.W., K.W., A.C., C.T.G.) and Arthritis and Clinical Immunology Research Program (S.T., M.C., S.K.), Oklahoma Medical Research Foundation. National Heart and Lung Institute, Imperial College London, United Kingdom (S.M.-A., N.D., L.O.-A., A.V.S., D.O.H., G.M.B., A.M.R.). Division of Nephrology and Hypertension, Feinberg Cardiovascular Research Institute, Northwestern University, Chicago, IL (R.P.S.). Department of Cell Biology, University of Oklahoma Health Sciences Center (C.T.G.). Now with Molecular and Clinical Sciences Institute, St. George's University of London, United Kingdom (S.M.-A.). Now with Ben May Department for Cancer Research, University of Chicago, IL (K.K.). Now with Queen Mary University, London, United Kingdom (N.D.). Now with JJC Center for Developmental Neurobiology, King's College London, United Kingdom (L.O.-A.). Now with Department of Pathology, Robert H. Lurie Comprehensive Cancer Center, Northwestern University, Chicago, IL (R.P.S.).

Acknowledgments

The authors would like to thank Justin C. Mason (Imperial College London) for his constant support and advice. C.M. Schafer, S. Martin-Almedina, G.M. Birdsey, A.M. Randi, and C.T. Griffin designed the study and interpreted the results. C.M. Schafer, S. Martin-Almedina, K. Kurylowicz, N. Dufton, L. Osuna-Almagro, M.-L. Wu, C.F. Johnson, A.V. Shah, A. Buxton, E. Willis, and K. Wheeler performed the experiments and data analysis and contributed to the interpretation of results. S. Turner, M. Chlebicz, and S. Kovats performed the intratracheal influenza infections. R.P. Scott performed and interpreted the transmission electron microscopy. D.O. Haskard contributed to the study design and edited the manuscript. C.M. Schafer wrote the manuscript with the help of A.M. Randi and C.T. Griffin. All other authors edited the manuscript.

Sources of Funding

This work was supported by grants from the National Institutes of Health (HL144605 and HL119501), the British Heart Foundation (PG/10/94/28651, RG/11/17/29256, and RG/17/4/32662), and the American Lung Association (CA-831087) and by Oklahoma Medical Research Foundation institutional support.

Disclosures

None.

Supplemental Material

Figures S1–S6
Tables S1–S4
Major Resources Table
ARRIVE Guidelines

REFERENCES

1. Schulte W, Bernhagen J, Bucala R. Cytokines in sepsis: potent immunoregulators and potential therapeutic targets—an updated view. *Mediat Inflamm*. 2013;2013:1–16.
2. Chaudhry H, Zhou J, Zhong Y, Ali MM, McGuire F, Nagarkatti PS, Nagarkatti M. Role of cytokines as a double-edged sword in sepsis. *Vivo Athens Greece*. 2013;27:669–684.
3. Joffre J, Hellman J, Ince C, Ait-Oufella H. Endothelial responses in sepsis. *Am J Resp Crit Care*. 2019;0:361–370.
4. Ince C, Mayeux PR, Nguyen T, Gomez H, Kellum JA, Ospina-Tascón GA, Hernandez G, Murray P, De Backer D; ADQI XIV Workgroup. The endothelium in sepsis. *Shock*. 2016;45:259–270. doi: 10.1097/SHK.0000000000000473
5. Muller WA. Leukocyte-endothelial cell interactions in the inflammatory response. *Lab Invest*. 2002;82:521–533. doi: 10.1038/labinvest.3780446
6. Goldenberg NM, Steinberg BE, Slutsky AS, Lee WL. Broken barriers: a new take on sepsis pathogenesis. *Sci Transl Med*. 2011;3:88ps25–88ps25. doi: 10.1126/scitranslmed.3002011
7. Aslan A, van Meurs M, Moser J, Popa ER, Jongman RM, Zwiers PJ, Molema G, Zijlstra JG. Organ-specific differences in endothelial permeability-regulating molecular responses in mouse and human sepsis. *Shock*. 2017;48:69–77. doi: 10.1097/SHK.0000000000000841
8. Matuschak GM, Lechner AJ. Acute lung injury and the acute respiratory distress syndrome: pathophysiology and treatment. *Mo Med*. 2010;107:252–258.
9. Parker JC. Acute lung injury and pulmonary vascular permeability: use of transgenic models. *Compr Physiol*. 2011;1:835–882. doi: 10.1002/cphy.c100013
10. Kor DJ, Warner DO, Carter RE, Meade LA, Wilson GA, Li M, Hamersma MJ, Hubmayr RD, Mauermann WJ, Gajic O. Extravascular lung water and pulmonary vascular permeability index as markers predictive of postoperative acute respiratory distress syndrome. *Crit Care Med*. 2015;43:665–673. doi: 10.1097/CCM.0000000000000765
11. Gonzales JN, Lucas R, Verin AD. The acute respiratory distress syndrome: mechanisms and perspective therapeutic approaches. *Austin J Vasc Medicine*. 2015;2:1009.
12. Teuwen L-A, Geldhof V, Pasut A, Carmeliet P. COVID-19: the vasculature unleashed. *Nat Rev Immunol*. 2020;20:389–391. doi: 10.1038/s41577-020-0343-0

13. Varga Z, Flammer AJ, Steiger P, Haberecker M, Andermatt R, Zinkernagel AS, Mehra MR, Schuepbach RA, Ruschitzka F, Moch H. Endothelial cell infection and endotheliitis in COVID-19. *Lancet*. 2020;395:1417–1418. doi: 10.1016/S0140-6736(20)30937-5
14. Angus DC, Linde-Zwirble WT, Lidicker J, Clermont G, Carcillo J, Pinsky MR. Epidemiology of severe sepsis in the United States: analysis of incidence, outcome, and associated costs of care. *Crit Care Med*. 2001;29:1303–1310. doi: 10.1097/00003246-200107000-00002
15. Opal SM, Poll T. Endothelial barrier dysfunction in septic shock. *J Intern Med*. 2015;277:277–293. doi: 10.1111/joim.12331
16. Opal SM, Dellinger RP, Vincent J-L, Masur H, Angus DC. The next generation of sepsis clinical trial designs: what is next after the demise of recombinant human activated protein C?*. *Crit Care Med*. 2014;42:1714–1721. doi: 10.1097/CCM.0000000000000325
17. Lucas R, Verin AD, Black SM, Catravas JD. Regulators of endothelial and epithelial barrier integrity and function in acute lung injury. *Biochem Pharmacol*. 2009;77:1763–1772. doi: 10.1016/j.bcp.2009.01.014
18. Shah AV, Birdsey GM, Peghaire C, Pitulescu ME, Dufton NP, Yang Y, Weinberg I, Osuna Almagro L, Payne L, Mason JC, et al. The endothelial transcription factor ERG mediates angiopoietin-1-dependent control of Notch signalling and vascular stability. *Nat Commun*. 2017;8:16002. doi: 10.1038/ncomms16002
19. Shah AV, Birdsey GM, Randi AM. Regulation of endothelial homeostasis, vascular development and angiogenesis by the transcription factor ERG. *Vasc Pharmacol*. 2016;86:3–13. doi: 10.1016/j.vph.2016.05.003
20. Yuan L, Nikolova-Krstevski V, Zhan Y, Kondo M, Bhasin M, Varghese L, Yano K, Carman CV, Aird WC, Oettgen P. Antiinflammatory effects of the ETS factor ERG in endothelial cells are mediated through transcriptional repression of the interleukin-8 gene. *Circ Res*. 2009;104:1049–1057. doi: 10.1161/CIRCRESAHA.108.190751
21. Yuan L, Bras AL, Sacharidou A, Itagaki K, Zhan Y, Kondo M, Carman CV, Davis GE, Aird WC, Oettgen P. ETS-related gene (ERG) controls endothelial cell permeability via transcriptional regulation of the claudin 5 (CLDN5) gene. *J Biol Chem*. 2012;287:6582–6591. doi: 10.1074/jbc.M111.300236
22. Looney AP, Han R, Stawski L, Marden G, Iwamoto M, Trojanowska M. Synergistic role of endothelial ERG and FLI1 in mediating pulmonary vascular homeostasis. *Am J Resp Cell Mol*. 2017;57:121–131. doi: 10.1165/rcmb.2016-0200OC
23. Caporarello N, Lee J, Pham TX, Jones DL, Guan J, Link PA, Meridew JA, Marden G, Yamashita T, Osborne CA, et al. Dysfunctional ERG signaling drives pulmonary vascular aging and persistent fibrosis. *Nat Commun*. 2022;13:4170. doi: 10.1038/s41467-022-31890-4
24. Mazzotta C, Marden G, Farina A, Bujor A, Trojanowski MA, Trojanowska M. FLI1 and ERG protein degradation is regulated via cathepsin B lysosomal pathway in human dermal microvascular endothelial cells. *Microcirculation*. 2021;28:e12660. doi: 10.1111/micc.12660
25. D'Amico G, Fernandez I, Gómez-Escudero J, Kim H, Maniati E, Azman MS, Mardakheh FK, Serrels B, Serrels A, Parsons M, et al. ERG activity is regulated by endothelial FAK coupling with TRIM25/USP9x in vascular patterning. *Development*. 2022;149:dev200528. doi: 10.1242/dev.200528
26. Robson MJ, Zhu C-B, Quinlan MA, Botschner DA, Baganz NL, Lindler KM, Thome JG, Hewlett WA, Blakely RD. Generation and characterization of mice expressing a conditional allele of the interleukin-1 receptor type 1. *PLoS One*. 2016;11:e0150068. doi: 10.1371/journal.pone.0150068
27. Pasparakis M, Alexopoulou L, Episkopou V, Kollias G. Immune and inflammatory responses in TNF alpha-deficient mice: a critical requirement for TNF alpha in the formation of primary B cell follicles, follicular dendritic cell networks and germinal centers, and in the maturation of the humoral immune response. *J Exp Medicine*. 1996;184:1397–1411. doi: 10.1084/jem.184.4.1397
28. Wang Y, Nakayama M, Pitulescu ME, Schmidt TS, Bochenek ML, Sakakibara A, Adams S, Davy A, Deutsch U, Lüthi U, et al. Ephrin-B2 controls VEGF-induced angiogenesis and lymphangiogenesis. *Nature*. 2010;465:483–486. doi: 10.1038/nature09002
29. Alva JA, Zovein AC, Monvoisin A, Murphy T, Salazar A, Harvey NL, Carmeliet P, Iruela-Arispe ML. VE-Cadherin-Cre-recombinase transgenic mouse: a tool for lineage analysis and gene deletion in endothelial cells. *Dev Dynam*. 2006;235:759–767. doi: 10.1002/dvdy.20643
30. Kisanuki YY, Hammer RE, Miyazaki J, Williams SC, Richardson JA, Yanagisawa M. Tie2-Cre transgenic mice: a new model for endothelial cell-lineage analysis in vivo. *Dev Biol*. 2001;230:230–242. doi: 10.1006/dbio.2000.0106
31. Ohta Y, Okabe T, Larmour C, Di Rocco A, Maijenburg MW, Phillips A, Speck NA, Wakitani S, Nakamura T, Yamada Y, et al. Articular cartilage endurance and resistance to osteoarthritic changes require transcription factor Erg. *Arthritis Rheumatol*. 2015;67:2679–2690. doi: 10.1002/art.39243
32. Birdsey GM, Shah AV, Dufton N, Reynolds LE, Osuna Almagro L, Yang Y, Aspalter IM, Khan ST, Mason JC, Dejana E, et al. The endothelial transcription factor ERG promotes vascular stability and growth through Wnt/β-catenin signaling. *Dev Cell*. 2015;32:82–96. doi: 10.1016/j.devcel.2014.11.016
33. Yardeni T, Eckhaus M, Morris HD, Huizing M, Hoogstraten-Miller S. Retro-orbital injections in mice. *Lab Animal*. 2011;40:155–160. doi: 10.1038/laban0511-155
34. Morales-Nebreda L, Chi M, Lecuona E, Chandel NS, Dada LA, Ridge K, Soberanes S, Nigdelioglu R, Sznajder JI, Mutlu GM, et al. Intratracheal administration of influenza virus is superior to intranasal administration as a model of acute lung injury. *J Virol Methods*. 2014;209:116–120. doi: 10.1016/j.jviromet.2014.09.004
35. Schneider CA, Rasband WS, Eliceiri KW. NIH image to ImageJ: 25 years of image analysis. *Nat Methods*. 2012;9:671–675. doi: 10.1038/nmeth.2089
36. Birdsey GM, Dryden NH, Amsellem V, Gebhardt F, Sahnan K, Haskard DO, Dejana E, Mason JC, Randi AM. Transcription factor Erg regulates angiogenesis and endothelial apoptosis through VE-cadherin. *Blood*. 2008;111:3498–3506. doi: 10.1182/blood-2007-08-105346
37. McLaughlin F, Ludbrook VJ, Kola I, Campbell CJ, Randi AM. Characterisation of the tumour necrosis factor (TNF)-(alpha) response elements in the human ICAM-2 promoter. *J Cell Sci*. 1999;112(pt 24):4695–4703. doi: 10.1242/jcs.112.24.4695
38. Lecker SH, Goldberg AL, Mitch WE. Protein degradation by the ubiquitin–proteasome pathway in normal and disease states. *J Am Soc Nephrol*. 2006;17:1807–1819. doi: 10.1681/ASN.2006010083
39. Schafer CM, Sheikh MO, Zhang D, West CM. Novel regulation of Skp1 by the dictyostelium AgtA α-galactosyltransferase involves the Skp1-binding activity of its WD40 repeat domain. *J Biol Chem*. 2014;289:9076–9088. doi: 10.1074/jbc.M113.528679
40. Cleuren ACA, van der Ent MA, Jiang H, Hunker KL, Yee A, Siemieniak DR, Molema G, Aird WC, Ganesh SK, Ginsburg D. The in vivo endothelial cell translatome is highly heterogeneous across vascular beds. *Proc National Acad Sci USA*. 2019;116:201912409.
41. Medvar B, Raghuram V, Pisitkun T, Sarkar A, Knepper MA. Comprehensive database of human E3 ubiquitin ligases: application to aquaporin-2 regulation. *Physiol Genomics*. 2016;48:502–512. doi: 10.1152/physiolgenomics.00031.2016
42. Wang S, Kollipara RK, Humphries CG, Ma S-H, Hutchinson R, Li R, Siddiqui J, Tomlins SA, Raj GV, Kittler R. The ubiquitin ligase TRIM25 targets ERG for degradation in prostate cancer. *Oncotarget*. 2016;7:64921–64931. doi: 10.18632/oncotarget.11915
43. Gan W, Dai X, Lunardi A, Li Z, Inuzuka H, Liu P, Varmeh S, Zhang J, Cheng L, Sun Y, et al. SPOP promotes ubiquitination and degradation of the ERG oncoprotein to suppress prostate cancer progression. *Mol Cell*. 2015;59:917–930. doi: 10.1016/j.molcel.2015.07.026
44. Gao R, Bhatnagar J, Blau DM, Greer P, Rollin DC, Denison AM, Deleon-Carnes M, Shieh W-J, Sambhara S, Tumpey TM, et al. Cytokine and chemokine profiles in lung tissues from fatal cases of 2009 pandemic influenza A (H1N1). *Am J Pathology*. 2013;183:1258–1268. doi: 10.1016/j.ajpath.2013.06.023
45. Kalna V, Yang Y, Peghaire C, Frudd K, Hannah R, Shah AV, Almagro LO, Boyle JJ, Göttgens B, Ferrer J, et al. The transcription factor ERG regulates super-enhancers associated with an endothelial-specific gene expression program. *Circ Res*. 2019;124:1337–1349. doi: 10.1161/CIRCRESAHA.118.313788
46. Augustin HG, Koh GY, Thurston G, Alitalo K. Control of vascular morphogenesis and homeostasis through the angiopoietin–Tie system. *Nat Rev Mol Cell Bio*. 2009;10:165–177. doi: 10.1038/nrm2639
47. Thamm K, Schrimpf C, Retzlaff J, Idowu TO, van Meurs M, Zijlstra JG, Ghosh CC, Zeitvogel J, Werfel TA, Haller H, et al. Molecular regulation of acute Tie2 suppression in sepsis. *Crit Care Med*. 2018;46:e928–e936. doi: 10.1097/CCM.0000000000003269
48. van der Heijden M, Amerongen GPN, Chedamni S, van Hinsbergh VW, Groeneveld AJ. The angiopoietin-Tie2 system as a therapeutic target in sepsis and acute lung injury. *Expert Opin Ther Tar*. 2009;13:39–53. doi: 10.1517/14728220802626256
49. Parikh SM. Dysregulation of the angiopoietin–Tie-2 axis in sepsis and ARDS. *Virulence*. 2013;4:517–524. doi: 10.4161/viru.24906
50. Parikh SM. Angiopoietins and Tie2 in vascular inflammation. *Curr Opin Hematol*. 2017;24:432–438. doi: 10.1097/MOH.0000000000000361
51. Ghosh CC, David S, Zhang R, Berghelli A, Milam K, Higgins SJ, Hunter J, Mukherjee A, Wei Y, Tran M, et al. Gene control of tyrosine kinase TIE2

and vascular manifestations of infections. *Proc National Acad Sci USA*. 2016;113:2472–2477. doi: 10.1073/pnas.1519467113
52. Milam KE, Parikh SM. The angiopoietin-Tie2 signaling axis in the vascular leakage of systemic inflammation. *Tissue Barriers*. 2014;3:e957508. doi: 10.4161/21688362.2014.957508
53. Dryden NH, Sperone A, Martin-Almedina S, Hannah RL, Birdsey GM, Khan ST, Layhadi JA, Mason JC, Haskard DO, Göttgens B, et al. The transcription factor Erg controls endothelial cell quiescence by repressing activity of nuclear factor (NF)-κB p65*. *J Biological Chem*. 2012;287:12331–12342. doi: 10.1074/jbc.M112.346791
54. Sperone A, Dryden NH, Birdsey GM, Madden L, Johns M, Evans PC, Mason JC, Haskard DO, Boyle JJ, Paleolog EM, et al. The transcription factor Erg inhibits vascular inflammation by repressing NF-κB activation and proinflammatory gene expression in endothelial cells. *Arterioscler Thromb Vasc Biol*. 2011;31:142–150. doi: 10.1161/ATVBAHA.110.216473
55. Alon R, Sportiello M, Kozlovski S, Kumar A, Reilly EC, Zarbock A, Garbi N, Topham DJ. Leukocyte trafficking to the lungs and beyond: lessons from influenza for COVID-19. *Nat Rev*. 2021;21:49–64. doi: 10.1038/s41577-020-00470-2
56. Aird WC. The role of the endothelium in severe sepsis and multiple organ dysfunction syndrome. *Blood*. 2003;101:3765–3777. doi: 10.1182/blood-2002-06-1887
57. Shao Y, Saredy J, Yang WY, Sun Y, Lu Y, Saaoud F, Drummer C 4th, Johnson C, Xu K, Jiang X, et al. Vascular endothelial cells and innate immunity. *Arterioscler Thromb Vasc Biol*. 2020;40:e138–e152. doi: 10.1161/ATVBAHA.120.314330
58. Donovan JA, Koretzky GA. CD45 and the immune response. *J Am Soc Nephrol Jasn*. 1993;4:976–985. doi: 10.1681/ASN.V44976
59. Gee MH, Albertine KH. Neutrophil-endothelial cell interactions in the lung. *Annu Rev Physiol*. 1993;55:227–248. doi: 10.1146/annurev.ph.55.030193.001303
60. Abraham E. Neutrophils and acute lung injury. *Crit Care Med*. 2003;31:S195–S199. doi: 10.1097/01.CCM.0000057843.47705.E8
61. Rossaint J, Zarbock A. Tissue-specific neutrophil recruitment into the lung, liver, and kidney. *J Innate Immun*. 2013;5:348–357. doi: 10.1159/000345943
62. Fleischmann C, Scherag A, Adhikari NKJ, Hartog CS, Tsaganos T, Schlattmann P, Angus DC, Reinhart K; International Forum of Acute Care Trialists. Assessment of global incidence and mortality of hospital-treated sepsis. Current estimates and limitations. *Am J Resp Crit Care Med*. 2016;193:259–272. doi: 10.1164/rccm.201504-0781OC
63. Hotchkiss RS, Moldawer LL, Opal SM, Reinhart K, Turnbull IR, Vincent J-L. Sepsis and septic shock. *Nat Rev Dis Primers*. 2016;2:16045. doi: 10.1038/nrdp.2016.45
64. Thompson BT, Chambers RC, Liu KD. Acute respiratory distress syndrome. *New Engl J Medicine*. 2017;377:562–572. doi: 10.1056/NEJMra1608077
65. Kim W-Y, Hong S-B. Sepsis and acute respiratory distress syndrome: recent update. *Tuberc Respir Dis*. 2016;79:53–57. doi: 10.4046/trd.2016.79.2.53
66. Matthay MA, Zemans RL, Zimmerman GA, Arabi YM, Beitler JR, Mercat A, Herridge M, Randolph AG, Calfee CS. Acute respiratory distress syndrome. *Nat Rev Dis Primers*. 2019;5:18. doi: 10.1038/s41572-019-0069-0
67. Luyt C-E, Combes A, Trouillet J-L, Nieszkowska A, Chastre J. Virus-induced acute respiratory distress syndrome: epidemiology, management and outcome. *Press Medicale Paris France 1983*. 2011;40:e561–e568. doi: 10.1016/j.lpm.2011.05.027
68. Prohaska S, Henn P, Wenz S, Frauenfeld L, Rosenberger P, Haeberle HA. A case report of fatal disseminated fungal sepsis in a patient with ARDS and extracorporeal membrane oxygenation. *Bmc Anesthesiol*. 2020;20:107. doi: 10.1186/s12871-020-01031-9
69. Silva L, Garcia L, Oliveira B, Tanita M, Festti J, Cardoso L, Lavado L, Grion C. Acute respiratory distress syndrome in burn patients: incidence and risk factor analysis. *Ann Burn Fire Disasters*. 2015;29:178–182.
70. Torre VD, Badenes R, Corradi F, Racca F, Lavinio A, Matta B, Bilotta F, Robba C. Acute respiratory distress syndrome in traumatic brain injury: how do we manage it? *J Thorac Dis*. 2017;9:5368–5381. doi: 10.21037/jtd.2017.11.03
71. Wilson KC, Saukkonen JJ. Acute respiratory failure from abused substances. *J Intensive Care Med*. 2004;19:183–193. doi: 10.1177/0885066604263918
72. Zhou MT, Chen CS, Chen BC, Zhang QY, Andersson R. Acute lung injury and ARDS in acute pancreatitis: mechanisms and potential intervention. *World J Gastroentero*. 2010;16:2094–2099. doi: 10.3748/wjg.v16.i17.2094
73. An J, Ren S, Murphy SJ, Dalangood S, Chang C, Pang X, Cui Y, Wang L, Pan Y, Zhang X, et al. Truncated ERG oncoproteins from TMPRSS2-ERG fusions are resistant to SPOP-mediated proteasome degradation. *Mol Cell*. 2015;59:904–916. doi: 10.1016/j.molcel.2015.07.025
74. Ayala G, Frolov A, Chatterjee D, He D, Hilsenbeck S, Ittmann M. Expression of ERG protein in prostate cancer: variability and biological correlates. *Endocr Relat Cancer*. 2015;22:277–287. doi: 10.1530/ERC-14-0586
75. Xiaoli L, Wujun Z, Jing L. Blocking of tripartite motif 8 protects against lipopolysaccharide (LPS)-induced acute lung injury by regulating AMPKα activity. *Biochem Biophys Res Commun*. 2019;508:701–708. doi: 10.1016/j.bbrc.2018.11.072
76. Seong BKA, Dharia NV, Lin S, Donovan KA, Chong S, Robichaud A, Conway A, Hamze A, Ross L, Alexe G, et al. TRIM8 modulates the EWS/FLI oncoprotein to promote survival in Ewing sarcoma. *Can Cell*. 2021;39:1262–1278. doi: 10.1016/j.ccell.2021.07.003
77. Jambusaria A, Hong Z, Zhang L, Srivastava S, Jana A, Toth PT, Dai Y, Malik AB, Rehman J. Endothelial heterogeneity across distinct vascular beds during homeostasis and inflammation. *Elife*. 2020;9:e51413. doi: 10.7554/eLife.51413
78. Schafer CM, Gurley JM, Kurylowicz K, Lin PK, Chen W, Elliott MH, Davis GE, Bhatti F, Griffin CT. An inhibitor of endothelial ETS transcription factors promotes physiologic and therapeutic vessel regression. *Proc National Acad Sci USA*. 2020;117:26494–26502. doi: 10.1073/pnas.2015980117
79. Peghaire C, Dufton NP, Lang M, Salles-Crawley II, Ahnström J, Kalna V, Raimondi C, Pericleous C, Inuabasi L, Kiseleva R, et al. The transcription factor ERG regulates a low shear stress-induced anti-thrombotic pathway in the microvasculature. *Nat Commun*. 2019;10:5014. doi: 10.1038/s41467-019-12897-w
80. Dufton NP, Peghaire CR, Osuna-Almagro L, Raimondi C, Kalna V, Chauhan A, Webb G, Yang Y, Birdsey GM, Lalor P, et al. Dynamic regulation of canonical TGFβ signalling by endothelial transcription factor ERG protects from liver fibrogenesis. *Nat Commun*. 2017;8:895. doi: 10.1038/s41467-017-01169-0
81. Nagai N, Ohguchi H, Nakaki R, Matsumura Y, Kanki Y, Sakai J, Aburatani H, Minami T. Downregulation of ERG and FLI1 expression in endothelial cells triggers endothelial-to-mesenchymal transition. *PLoS Genet*. 2018;14:e1007826. doi: 10.1371/journal.pgen.1007826
82. Kruse EA, Loughran SJ, Baldwin TM, Josefsson EC, Ellis S, Watson DK, Nurden P, Metcalf D, Hilton DJ, Alexander WS, et al. Dual requirement for the ETS transcription factors Fli-1 and Erg in hematopoietic stem cells and the megakaryocyte lineage. *Proc National Acad Sci USA*. 2009;106:13814–13819. doi: 10.1073/pnas.0906556106